EXCITED STATES OF THE MIRROR NUCLEI

Be^7 AND Li^7

Thesis by

Alfred Bruce Brown, Jr.

In Partial Fulfillment of the Requirements

For the Degree of

Doctor of Philosophy

California Institute of Technology

Pasadena, California

1950

ACKNOWLEDGMENTS

The operation of experimental apparatus as complex as that in use in the Kellogg Radiation Laboratory is often more than can be done by one person. In this case, at least three were necessary to control the Van de Graaff accelerator, the magnetic spectrometer, and the counters, and to record data; I am indebted to Professor C. C. Lauritsen, Professor W. A. Fowler, and Dr. C. Y. Chao for taking part in this work.

I am indebted for financial aid to the Office of Naval Research, to the Ethyl Corporation for a fellowship in 1947-1948, and to the California Institute of Technology for graduate assistantships in the two succeeding years.

I wish to thank Professor Lauritsen and Professor Fowler for suggesting and supervising the problem, and for the opportunity to work with them. Discussions of the problem with Professor Fowler, Professor R. F. Christy, and Mr. R. G. Thomas have been very helpful, and their interest is appreciated.

ABSTRACT

A low energy group of alpha particles has been found to result from the reaction $B^{10}(p\ \alpha)Be^{7*}$, indicating the existence of an excited state of Be^7. Observation of this group and separation of the group from protons elastically scattered by the thin B^{10} targets was made possible through high resolution magnetic analysis supplemented by absorption techniques. The excitation of the state is 0.434 $\pm$ .005 Mev, and the Q-value of the reaction to the ground state is 1.148 $\pm$ .006 Mev. The Q-value of the reaction to the excited state is thus 0.714 $\pm$ .008 Mev. On the basis of approximately equal neutron-neutron and proton-proton forces, the energy difference between the ground states of Li^7 and Be^7 can be accounted for as electrostatic energy, using a reasonable value of average separation of protons in the two nuclei. The energy difference between the state in Be^7 at 0.434 Mev and the state in Li^7 at 0.478 Mev can be similarly accounted for, if a small increase in the size of the nuclei over their size in the ground state is assumed. These results indicate that the ground states of the two nuclei may be considered corresponding states, and that the excited states may also be so considered. In the reaction to the excited state in Be^7 a resonance of about 0.28 Mev width exists at 1.51 Mev proton energy, and is observed in the yield of both alpha particles and gamma rays. In the reaction to the ground state there is a resonance 0.55 Mev wide at 1.06 Mev proton energy, and there is some indication of another at about 1.5 Mev.

TABLE OF CONTENTS

PART I - INTRODUCTION

If in two nuclear species the number of protons in the nucleus of each is equal to the number of neutrons in the nucleus of the other, they are known as "mirror nuclei". Several such pairs of nuclei are known among the light elements, examples being H^3 and He^3, Li^7 and Be^7, B^{11} and C^{11}, and C^{13} and N^{13}. Examples having even mass number are also known, such as Be^{10} and C^{10}. In general, at least one of the nuclei of the pair is radioactive.

Study of the excited states of mirror nuclei may lead to some information concerning nuclear forces. The assumption is made that the nuclear forces are only between pairs of particles; that is, that the force on any particle may be expressed as the vector sum of the forces on it due to the presence of each of the other nuclear particles. If this assumption is correct, and if the force between two neutrons is approximately the same as the force between two protons, except for the relatively small electrostatic repulsion of the protons, then two mirror nuclei should have corresponding quantum states. The number of neutron-proton pair combinations which can be found in one nucleus is the same as in the other, so the result is independent of the neutron-proton force; the number of proton-proton combinations in each nucleus is the same as the number of neutron-neutron combinations in the other.

The electrostatic forces are much less strong than the nuclear forces, and may be considered as causing only a small perturbation in the quantum states. The electrostatic energy

due to the mutual repulsion of the protons in a nucleus may be expressed[1] as:

$$E_c = \frac{Z(Z-1)}{2} e^2 \overline{(1/r)} \qquad (1)$$

where Z is the number of protons in the nucleus, e the charge on a proton, and $\overline{(1/r)}$ is the average of the reciprocal of the distance between two protons in the nucleus. Fowler, Delsasso, and Lauritsen give 3.5×10^{12} cm^{-1} for $\overline{(1/r)}$ for nuclei having mass between 9 and 20 atomic mass units. With this value as an estimate for mass 7, there result

$$E_c(Li^7) = 1.52 \text{ Mev}$$
$$E_c(Be^7) = 3.03 \text{ Mev}$$

The energy of nuclear quantum states will, of course, be somewhat changed by the electrostatic repulsion, and in two mirror nuclei will be changed by different amounts.

The nuclei selected for study, Li^7 and Be^7, were chosen for a number of reasons. Li^7 has been extensively studied for many years[2] and two excited states are known, one at 0.478 Mev and the other at 7.38 Mev. The absence of other states below a few Mev simplifies the problem. Recently Inglis[3] has verified that no other state below 2.5 Mev is strongly produced in the reaction $Be^9(d\,\alpha)Li^7$. However, no excited states had been found in Be^7 to correspond to the states in Li^7, even though the nucleus had often been produced in nuclear reactions such as $B^{10}(p\,\alpha)Be^7$, $Li^7(p\,n)Be^7$, and $Li^6(d\,n)Be^7$. For this work the reaction used was $B^{10}(p\,\alpha)Be^7$, for two reasons. The reaction is initiated by and produces charged particles, making precise energy measurements easy. The Q-value of the reaction leading to the ground state of Be^7 had been measured as 1.148 Mev[4], so

the Q-value of a reaction leaving Be^7 excited by about 0.45 Mev would be about 700 kev; the reaction could therefore be carried out and the product particles studied with the equipment available.

If the assumptions made above about nuclear forces are correct, the energy difference between corresponding states of mirror nuclei gives an indication of the nuclear size. Because the electrostatic forces are so much smaller than the nuclear forces, comparison of this size estimate with those derived from other considerations serves as a significant test of the assumptions.

One can express the total energy of the ground states of Li^7 and Be^7 in the following manner:

$$Li^7 = 4n^1 + 3H^1 + U_n + E_c(Li^7) \qquad (2)$$

$$Be^7 = 3n^1 + 4H^1 + U_n + E_c(Be^7) \qquad (3)$$

where the symbols Li^7, Be^7, n^1, and H^1 indicate the mass energy, U_n is the potential energy due to nuclear forces and is a negative number, and $E_c(Li^7)$ and $E_c(Be^7)$ are the Coulomb energies. If the nuclei are in corresponding states, then U_n is the same for the two nuclei. Equations 2 and 3 can be combined to express the energy difference of the ground states of Li^7 and Be^7 in terms of the neutron-proton mass difference and the difference of Coulomb energies.

$$Be^7 - Li^7 = -(n^1 - H^1) + E_c(Be^7) - E_c(Li^7) \qquad (4)$$

The same quantity can be expressed in terms of the experimentally determined Q-values of $B^{10}(p\,\alpha)Be^7$ and $B^{10}(n\,\alpha)Li^7$:

$$B^{10} + H^1 = Be^7 + He^4 + Q_1 \qquad (5)$$

$$B^{10} + n^1 = Li^7 + He^4 + Q_2 \qquad (6)$$

and therefore

$$Be^7 - Li^7 = -(n^1 - H^1) + Q_2 - Q_1 \tag{7}$$

$$E_c(Be^7) - E_c(Li^7) = Q_2 - Q_1 \tag{8}$$

Equation 1 can be used for $E_c(Be^7)$ and $E_c(Li^7)$, but for this to be useful it must first be shown that the same value of $\overline{(1/r)}$ can be used for the two nuclei. To do this, the reasoning of Feenberg and Goerzel[5] is used. Two quantities are defined: L_s, the average Coulomb interaction between two protons whose wave functions are symmetric in the space coordinates, and L_a, the corresponding interaction between two protons whose wave functions are antisymmetric in the space coordinates. Feenberg and Goerzel assumed that L_s and L_a are constant for a given isobaric series, although not necessarily equal. Then the Coulomb energies of Li^7 and Be^7 may be expressed in terms of L_s and L_a:

$$E_c(Li^7) = L_s + \tfrac{1}{2}(L_s + 3L_a) \tag{9}$$

$$E_c(Be^7) = 2L_s + (L_s + 3L_a) \tag{10}$$

Each of these two nuclei has equal numbers of L_s and L_a, so for each,

$$\overline{(1/r)} = \frac{\overline{(1/r_s)} + \overline{(1/r_a)}}{2} \tag{11}$$

The assumption of Feenberg and Goerzel is equivalent to assuming that $\overline{(1/r_s)}$ and $\overline{(1/r_a)}$ are the same for the two nuclei, though it is not assumed that they are equal to each other.

Substituting Equation 1 into Equation 8 for each of the two Coulomb energies gives

$$3e^2\overline{(1/r)} = Q_2 - Q_1 \tag{12}$$

This equation will be discussed further in Part VIII, when

values will be substituted for Q_2 and Q_1.

The development which led to Equation 4 can be followed for corresponding excited states, giving instead of Equation 4 the expression

$$Be^{7*} - Li^{7*} = -(n^1 - H^1) + E_c(Be^{7*}) - E_c(Li^{7*}) \qquad (13)$$

The total energies of the excited states of Be^7 and Li^7 can be expressed in terms of the ground states:

$$Be^{7*} - Li^{7*} = Be^7 - Li^7 + E_x(Be^{7*}) - E_x(Li^{7*}) \qquad (14)$$

where E_x is the excitation energy of the state. Combining Equations 1, 7, 13, and 14, we have

$$3e^2\overline{(1/r^*)} = Q_2 - Q_1 + E_x(Be^{7*}) - E_x(Li^{7*}) \qquad (15)$$

This equation will be discussed further in Part VIII, and r will be compared with r*.

PART II - THE EXPERIMENTAL ARRANGEMENTS

The protons for the bombardment were accelerated in the 1.6 Mev Van de Graaff accelerator[6] of the Kellogg Radiation Laboratory. The protons were analyzed for energy in an electrostatic analyzer[7] whose energy resolution is about .05% of the bombarding energy. The electrostatic analyzer was calibrated against the known resonance in the gamma ray yield from proton bombardment of fluorine at 873.5 kev. The resonance curve found from bombardment of a thin zinc fluoride target is shown in Figure 1. The ordinates are the readings of the potentiometer used, with a voltage divider, to measure the potential across the analyzer plates. The particle energy being proportional to the analyzer plate potential, it may be expressed as

C_eP, where C_e is a constant equal to 0.1240 kev/potentiometer division and P is the potentiometer reading. In making the calibration, corrections were made for relativistic mass change, the retarding potential on the target which reduced secondary electron emission, the rise of target potential during the run due to charging of the charge integrator condenser, and the carbon layer on the target. The last correction was quite small, as a liquid air trap was installed near the target chamber to reduce the amount of pump oil vapor there. It is believed that the proton energy was known to about 0.2%.

The targets were of four types: amorphous boron pressed on a copper strip one-sixteenth inch thick, boron evaporated on aluminum leaf, boric anhydride (B_2O_3) evaporated on aluminum leaf, and boric anhydride evaporated on copper strip. The thickness of the aluminum leaf was about 0.2 milligrams per square centimeter. The reasons for using the different types of targets will be discussed in the description of the experiments. In all cases the boron was the B^{10} isotope, obtained from the Atomic Energy Commission. The boric anhydride was evaporated using a small tantalum strip as a heating element. The evaporated boron targets were made in the hope of obtaining thin targets undiluted by oxygen; such targets would give greater yields of alpha particles. The heating element in the furnace was a strip of tungsten .005 inches thick, $\frac{1}{2}$ inch wide, and about $\frac{1}{2}$ inch long, and the currents were of the order of 150 amperes. The boron was spread directly on top of the tungsten strip. Since boron must be heated to about 2500° Centigrade before it evaporates appreciably and our evaporation times were several minutes, the

contamination from pump oil which struck the heating element and decomposed was not to be neglected. A liquid air trap was used to keep oil vapors from entering the target chamber, but the contamination was still serious. When the target was examined by the elastic scattering of protons, it was found that carbon and oxygen were present in amounts comparable to the boron. A precise analysis[8] by this method was not made because proton scattering from carbon and from boron shows anomalies in this region of proton energies, and experimental data on the cross section for proton scattering from carbon was not available. By comparing the yield of $B^{10}(p\ \alpha)Be^{7*}$ from one of the evaporated boron targets and from a target of boric anhydride, the boron target was found to be only about 40% boron. Results of the proton scattering indicate that most of the rest was carbon.

The gamma rays were detected by a Geiger-Müller counter made by the Radiation Counter Laboratories. The glass wall of the counter was thin, about 30 milligrams per square centimeter, and the cathode was a thin silver deposit on the glass wall. The effective length of the counter was 3 5/8 inches and its diameter was 23/32 inch. The counter was mounted in a lead cylinder 2 7/8 inches in diameter with a slot the width and length of the counter cut to admit the radiation. The hole for the counter was lined with an aluminum cylinder whose wall thickness was 3/32 inch.

Alpha particles and protons were detected by a scintillation counter built by Mr. A. V. Tollestrup; before reaching the counter the particles passed through a double-focusing magnetic spectrometer[9]. The momentum resolution of the spectrometer was 128,

determined from the widths of the profiles of thin targets and thin deposits of carbon (Figure 2). The spectrometer was calibrated by the elastic scattering of protons from carbon, boron, aluminum, and copper. The measurement of the magnetic field was made with the fluxmeter described in Reference 9. Classically, the energy of a particle which passes through the spectrometer is given by C_m/I^2, where I is the potentiometer reading (proportional to the fluxmeter current) and C_m is a constant depending on the charge and mass of the particle, and is equal to 1.765×10^6 kev millivolts^2 for alpha particles. The same corrections were made as in the calibration of the electrostatic analyzer, and in addition a correction was made for the effect of the relativistic mass change on the energy measurement by the spectrometer. It is believed that measurements made with the spectrometer of the energy of particles are uncertain by about 0.3%.

In those cases where protons of the same energy as the alpha particles were scattered into the spectrometer, the alpha particles were distinguished from the protons by aluminum foils whose total thickness was about 0.6 milligrams per square centimeter. Readings were taken with and without foils and the alpha particle counts calculated by subtraction. These foils were sufficient to stop nearly all the alpha particles up to about 900 kev, but above that energy the fraction of the alpha particles which emerged from the foils with sufficient energy to be counted was large enough to make the readings uncertain.

The spectrometer accepted particles emerging from the target at a mean angle of $137.8^\circ \pm 0.3^\circ$ with the direction of the proton

beam. This angle was measured[10] using a narrow slit at the entrance to the spectrometer. It was found that the total effective angular opening of the spectrometer in this direction was 6.6°.

PART III - EXCITATION ENERGY OF Be^{7*}

The excitation energy of the residual Be^7 was found by bombarding the boron target with known energy protons and observing the energy of the alpha particles emitted from the target at 137.8° in laboratory coordinates. The target used was evaporated B^{10} deposited on aluminum leaf, whose thickness was about 0.2 milligrams per square centimeter. In this part of the experiment it was necessary to have a target which was not too thick, so that when the reaction leading to the excited state of Be^7 was being run elastically scattered protons and alpha particles from the reaction leading to the ground state of Be^7 would not enter the spectrometer in too great numbers. The low energy group of alpha particles had less energy than scattered protons or alpha particles of the main group and ordinarily the spectrometer would distinguish between them; however, particles originating deep in the target or backing foil with high energy would in some cases lose enough energy in the target to emerge with the same amount as the particles being studied. The subtraction technique which was used for distinguishing between protons and alpha particles resulted in large statistical uncertainties if the number of protons became equal to or larger than the number of alpha particles. By using a thin target and thin backing foil, the protons were nearly all

of a few definite energies, determined by the bombarding energy and the masses of the scattering atoms. Since the alpha particle energy had a different dependence on the energy of the bombarding protons than did the energy of the elastically scattered protons, the reaction could be run at some bombarding energy at which few of the scattered protons had the same energy as the alpha particles. The impurity of the boron target did not affect the measurement of the Q-values, because determination of the absolute yield was not necessary.

The Q-value of the reaction to the ground state of Be^7 was calculated from the following expression:

$$Q = E_2(1 + M_2/M_3) - E_1(1 - M_1/M_3) - 2 \cos\theta\, (E_1E_2M_1M_2)^{\frac{1}{2}}/M_3 \quad (16)$$

In this equation and those following the subscript o refers to the target nucleus, 1 to the bombarding particle, 2 to the emitted particle which is observed, and 3 to the residual nucleus. Equation 16 is derived non-relativistically from conservation of energy and momentum, by substitution of

$$E_2 + E_3 - E_1 = Q \quad (17)$$

and

$$P_i^2 = 2M_iE_i \qquad (i = 1,2,3) \quad (18)$$

in the expression for the conservation of momentum

$$P_1^2 - 2P_1P_2 \cos\theta + P_2^2 = P_3^2 \quad (19)$$

and solving for Q. If, instead of the classical relation between momentum and kinetic energy given in Equation 18, the relativistic expression

$$P_i^2 = E_i^2/c^2 + 2E_iM_i = 2E_iM_i(1 + E_i/2M_ic^2) \qquad (20)$$

is used, each mass in Equation 16 is replaced by $M_i(1 + E_i/2M_ic^2)$. In this case E_3 is not replaced where it appears as a correction to M_3 by its value from Equation 17. In the reaction being studied, the relativistic correction amounts to much less than one kilovolt in any case, so the procedure adopted was to use approximate values for the kinetic energies, making the same correction for all bombarding energies. Relativistic corrections were made to the proton and alpha particle energies measured by the electrostatic analyzer and magnetic spectrometer in all cases.

In order to obtain an accurate value for the difference of the Q-values of the reactions to the ground state and to the excited state of Be^7, the alpha particles from the two reactions were observed at different bombarding energies, so chosen that the energies of the alpha particles were approximately the same. In this way the determination of the excitation energy of Be^{7*} was insensitive to errors of calibration of the magnetic spectrometer. The excitation of the excited state of Be^7 was found to be 0.434 ± .005 Mev, and the Q-value of $B^{10}(p\ \alpha)Be^7$, 1.148 ± .006 Mev. The Q-value is the average of eight determinations made by Chao, Lauritsen, and Tollestrup[4] and three determinations made by Professor Lauritsen, Professor Fowler, Dr. Chao, and myself. The difference between the Q-value of the reaction to the ground state of Be^7 and the excitation energy of Be^{7*} is the Q-value of $B^{10}(p\ \alpha)Be^{7*}$, which is therefore 0.714 ± .008 Mev.

The profiles of the alpha particles from $B^{10}(p\,\alpha)Be^{7*}$ and from $B^{10}(p\,\alpha)Be^{7}$ are shown in Figure 3. Since the target was neither much thinner nor much thicker to alpha particles than the spectrometer resolution, it was not correct to take either the peak of the curve or the point at which it reached half its maximum as the alpha particle energy. Estimation of the target thickness from the shape of the curve indicated that the most probably correct point is that at which the yield is 0.6 times the maximum, the target being nearly as thick as the spectrometer. Uncertainty in the fluxmeter reading corresponding to the alpha particle energy accounts for the majority of the uncertainty in the level excitation energy. Uncertainty in the target thickness affects all the I values the same way, and its effect is largely cancelled by using ΔI.

By writing Equation 16 once for the main group of alpha particles and once, using primes for the energies, for the low energy group and subtracting the second form from the first, one obtains:

$$\begin{aligned}\Delta Q &= Q - Q' \\ &= -\Delta E_2(1 + M_2/M_3) + \Delta E_1(1 - M_1/M_3) - \\ &\quad - 2\cos\Theta\,(M_1M_2)^{\frac{1}{2}}\left[(E_1E_2)^{\frac{1}{2}} - (E_1'E_2')^{\frac{1}{2}}\right]/M_3 \qquad (21)\end{aligned}$$

where $\Delta E_2 = E_2' - E_2$ and $\Delta E_1 = E_1' - E_1$. Substitution of C_eP for E_1 and C_m/I^2 for E_2 and insertion of the first order relativistic correction for E_2 in the first term and the exact relativistic correction for E_1 in the second term result in the equation:

$$\Delta Q = (1 + M_2/M_3)(C_m/I^2)\left[2(\Delta I/I) - 3(\Delta I/I)^2 + 4(\Delta I/I)^3 -\right.$$

$$- C_m 4(\Delta I/I)/2M_2c^2I^2\Big] +$$

$$+ (1 - M_1/M_3)C_e\Delta P(1 + C_e(P + P')/2M_1c^2) -$$

$$- 2\cos\theta\,(M_1M_2C_mC_e)^{\frac{1}{2}}(P^{\frac{1}{2}}/I - P'^{\frac{1}{2}}/I')/M_3 \qquad (22)$$

where $\Delta P = P' - P$ and $\Delta I = I' - I$. It is noteworthy that many of the corrections, such as the relativistic corrections in the last term, the correction for a carbon layer on the target and for the difference between target potential and ground, cancelled either entirely or to a degree which made their inclusion unnecessary. At least nine-tenths of the uncertainty in the final value for the excitation energy is due to lack of precision in ΔI. The uncertainty is of the order of 0.02 millivolts on the potentiometer in each reading, resulting in a probable error of 0.03 millivolts in the difference, ΔI. This indicates that the final excitation energy is uncertain by about 2.5 kev.

Each of the three readings for the main group was combined with each of the two readings for the low energy group in order to give as nearly as possible equal weight to each determination of a Q-value, and the resulting six values of ΔQ were averaged. The scatter of the results indicates that the probable error of the average is about 5 kev, and the estimate of uncertainty in I was probably too low. In finding ΔQ, it was not possible to use the eight earlier determinations of the Q-value of the reaction $B^{10}(p\,\alpha)Be^7$ because it was found that the calibration of the magnetic spectrometer had changed between the time those determinations were made and the time the first reliable work

was done on the low energy group of alpha particles. Table I summarizes the results on ΔQ.

Table 1

P	P'	I	I'	ΔQ
8000	12000	41.85	43.10	435.4 kev
8000	12400	41.85	42.75	441.0
7000	12000	42.88	43.10	429.7
7000	12400	42.88	42.75	435.2
7150	12000	42.73	43.10	429.8
7150	12400	42.73	42.75	435.3
			Average	434.4 $\pm$ 5

This result for the excitation energy of the state of Be^7 may be compared with the results obtained by other workers:

Table 2

Measurements of the Excitation Energy of Be^{7*}

Authors	Reaction	Energy
Lauritsen and Thomas[11]	$Li^6(d\ n)Be^7$, $B^{10}(p\ \alpha)Be^7$	429 ± 5 kev
Whaling and Butler[12]	$Li^6(d\ n)Be^7$	435 (possibly)
Gibson[13]	$Li^6(d\ n)Be^7$	450 ± 60
Johnson, Laubenstein, and Richards[14]	$Li^7(p\ n)Be^7$	435 ± 15
Grosskreutz and Mather[15][16]	$Li^7(p\ n)Be^7$	470 ± 70
Hamermesh and Hummel[17]	$Li^7(p\ n)Be^7$	428 ± 20
Freier, Rosen, and Stratton[18]	$Li^7(p\ n)Be^7$	428 ± 15
Hall[19]	$Li^7(p\ n)Be^7$	420 to 480
Burcham and Freeman[20]	$B^{10}(p\ \alpha)Be^7$	About 400
Van Patter, Sperduto, and Buechner[21]	$B^{10}(p\ \alpha)Be^7$	429

PART IV - THE CROSS SECTION OF $B^{10}(p\ \alpha)Be^{7}$

In connection with these studies, four cross sections were measured: the main group of alpha particles, the low energy group of alpha particles, the gamma rays from $B^{10}(p\ \alpha)Be^{7*}$, and the protons scattered elastically from B^{10}. The cross section of the main group of alpha particles was measured for proton energies from 615 kev to 1114 kev and from 1208 kev to 1585 kev. As will be described later, it was necessary to use different target arrangements in the two energy ranges to avoid scattered protons. Between 1114 kev and 1208 kev, with either target arrangement, excessive numbers of protons were scattered into the spectrometer with energies causing them to be counted, so that reliable data for the alpha particles could not be obtained.

For bombarding energies between 615 kev and 1114 kev, the target was made by evaporating on a copper strip a layer of boric anhydride thick enough to stop all protons. At these bombarding energies protons scattered elastically by heavy backing material have approximately the same energy as the alpha particles from the reaction being studied, and it is necessary to absorb them; for this reason the layer of boric anhydride was made thick. However, as the bombarding energy is increased in this range, the energy of the protons scattered from oxygen increases faster than the alpha particle energy and one comes to a point where their energies are nearly the same, and too many protons from the oxygen are scattered with the same energy as the alpha particles from the boron have. The target was deposited on a copper strip so the energy of

the bombarding protons, which was converted to heat when they were stopped, could be conducted away.

The cross section for this reaction when the target is thicker to the product particles than the spectrometer window is given by the expression

$$\sigma(\theta) = \frac{(\alpha^{++}/S)\,S}{V\,C \times 6.24 \times 10^{12}} \times \frac{\epsilon_{eff}}{2E_{20}} \times \frac{4\pi R}{\Delta\Omega_L}\left(\frac{d\Omega_C}{d\Omega_L}\right)^{-1} (1 + He^{+}/He^{++}) \qquad (23)$$

where $\sigma(\theta)$ is 4π times the cross section per unit solid angle observed at an angle θ with the incident beam, α^{++}/S is the number of counts observed on the mechanical register due to doubly charged alpha particles, S is the scale factor of the electronic scaler, and V and C are the potential in volts to which the current integrator capacitor was charged and the capacitance of that capacitor in microfarads. ϵ_{eff} is defined by Equation 28, E_{20} is the energy of the alpha particles as measured by the spectrometer, R is the momentum resolution of the spectrometer, $\Delta\Omega_L$ is the solid angle in which the spectrometer will accept particles leaving the target, and the last two factors are respectively the correction of solid angle from laboratory to center of mass coordinates and the correction to allow for those helium nuclei which are produced in the reaction but are not counted because they are only singly charged when they leave the target. The correction for singly-charged helium nuclei was obtained from a curve drawn by Mr. R. G. Thomas, for which I am indebted to him. It is included as Figure 4.

Equation 23 may be derived in the following way. The cross

section per unit solid angle for any reaction may be expressed

$$\frac{d\sigma}{d\Omega} = \frac{\text{Particles counted}}{\text{Bombarding particles} \times (\text{target nuclei/cm}^2) \times \Delta\Omega_c} \qquad (24)$$

In order to go from this equation to Equation 23, one replaces "Particles counted" by $(\alpha^{++}/S)S$, "Bombarding particles" by $V\ C \times 6.24 \times 10^{12}$, and $\Delta\Omega_c$, the solid angle in center of mass coordinates, by the corresponding solid angle in laboratory coordinates and the correction factor. One inserts the correction factor for singly charged helium nuclei and multiplies by 4π, obtaining an equivalent cross section for isotropic distribution of the product particles in center of mass coordinates. In addition, it is necessary to find an expression for "Target particles/cm^2", usually designated "nt".

When the target is thicker than the spectrometer window, the only particles entering the spectrometer and passing through it to the counter are those produced in reactions occurring in a certain lamina of the target, as shown in Figure 5. The lamina is defined by the energies E_2 and E_2'', which are the limits of the energy band accepted by the spectrometer at a given magnetic field value. As the protons pass through the lamina, they lose an amount of energy equal to

$$E_1 - E_1' = nt\ \epsilon_1 \qquad (25)$$

where ϵ_1 is the stopping cross section of the target per disintegrable nucleus for protons whose energy is the bombarding energy. Alpha particles produced at the back of the lamina have energies equal to

$$E_2' = E_2 - (E_1 - E_1')(\partial E_2/\partial E_1)$$

$$= E_2 - nt\,\epsilon_1(\partial E_2/\partial E_1) \qquad (26)$$

in which only the first two terms of the Taylor series are kept, and when the alpha particles reach the front of the lamina they have energies

$$E_2'' = E_2' - nt\,\epsilon_2 \cos\theta_1/\cos\theta_2 \qquad (27)$$

where ϵ_2 is the stopping cross section of the target per disintegrable nucleus for product particles of the given energy. Combining Equations 26 and 27, we arrive at the expression for the energy band accepted by the spectrometer:

$$\delta E_2 = E_2 - E_2'' = nt(\epsilon_1 \partial E_2/\partial E_1 + \epsilon_2 \cos\theta_1/\cos\theta_2)$$

$$= nt\ \epsilon_{eff} \qquad (28)$$

where ϵ_{eff} is defined by this equation. It is evident that ϵ_{eff} depends on the target material, the reaction, the bombarding energy, and the alignment of the proton beam and spectrometer with respect to the target.

Using the definition of the spectrometer resolution and the classical relation between momentum and kinetic energy, we have:

$$P_2/\delta P_2 = R = 2E_{20}/\delta E_{20} \qquad (29)$$

Substituting Equation 29 in Equation 28 and solving for nt, we have:

$$nt = 2E_{20}/\epsilon_{eff} R \qquad (30)$$

The derivation of Equation 23 is now complete.

It was found necessary to compute ϵ_{eff} in several materials for targets oriented at $\theta_1 = 28^\circ$. The computations were based on the data and equations of Livingston and Bethe[22], to be designated L & B. In all cases the quantity s, which is defined by Equation 764 (L & B) and is the ratio of the stopping cross section in the material of interest to that in air, was first found, and the stopping cross section in air was found from Figure 31, L & B. For boron and oxygen, Equation 749a of the reference was used to compute s; I and Z for air were taken equal to 80.5 volts and 7.22, respectively, and for the other materials I was taken proportional to Z. For carbon, L & B Figures 29, 30, and 33 gave the ratio of the stopping cross sections, while for aluminum the ratio was obtained from Table XLIX, page 272 of L & B, by graphical interpolation. The stopping cross section per B^{10} atom of a target made of more than one element was found as follows:

$$\epsilon = \epsilon_B + \sum_i n_i \epsilon_i / n_B \qquad (31)$$

where n_i is the number of "i" nuclei per cubic centimeter of the target. If the target is a compound, such as B_2O_3, the ratio n_i/n_B may be known precisely.

E_{20} was taken equal to C_m/I^2, the relativistic correction being obviously unnecessary.

The solid angle correction from center of mass to laboratory coordinates was made according to the following non-relativistic expression:

$$d\Omega_C/d\Omega_L = 2\beta\cos\theta_L + (1-\beta^2\sin^2\theta_L)^{\frac{1}{2}} +$$

$$+ \beta^2\cos^2\theta_L(1-\beta^2\sin^2\theta_L)^{-\frac{1}{2}} \qquad (32)$$

where

$$\beta = (M_1M_2E_{1L})^{\frac{1}{2}}/(MM_3Q + M_0M_3E_{1L})^{\frac{1}{2}} \qquad (33)$$

and $M = M_1 + M_0$. E_{1L} is the energy of the bombarding particle in laboratory coordinates at the point where the reaction takes place. This expression is somewhat more convenient than the usual one[23], since it uses the laboratory angle instead of the center of mass angle. In reducing data for an excitation curve, where the center of mass angle varies with the bombarding energy, the labor of computation is considerably reduced. It can be shown that the two formulas are equivalent, using the following expression to relate the angles:

$$\cos\theta_C = -\beta\sin^2\theta_L + (1-\beta^2\sin^2\theta_L)^{\frac{1}{2}}\cos\theta_L \qquad (34)$$

β is the same as before, and is the γ used by Schiff. Equations 32 and 34 are derived in the appendix.

The factor $4\pi R/\Delta\Omega_L$ is a constant of the spectrometer, and may be determined from any reaction whose cross section is already known. In this case the elastic scattering of protons from copper was used. The cross section was calculated from the Rutherford formula

$$\sigma(\theta) = (\pi e^4/4\sin^4(\theta_c/2))(Z_1Z_0/\alpha E_{1L})^2 \qquad (35)$$

where $\alpha = M_0/(M_1 + M_0)$.

The stopping cross section of copper was found by calculating its ratio to the stopping cross section of air from L & B Equations 749a and 764, and by using Figure 31 of the reference to find the stopping cross section of air. The bombarding energy was 1.478 Mev, and the constants Z and I for copper in Equation 749a were chosen to fit the data given in Table XLIX, page 272, L & B, at 1.17 and 2.09 Mev bombarding energy. $4\pi R/\Delta\Omega_L$ was found to be 2.933×10^5, with a statistical uncertainty of about ½%, and an uncertainty due to lack of knowledge of the stopping cross section of copper of a few per cent.

Returning to the discussion of the cross section measurements of the reaction $B^{10}(p\ \alpha)Be^7$ for bombarding energies between 615 and 1114 kev, we see that the only remaining quantity to be determined in Equation 23 is α^{++}/S. The technique of interposing aluminum foils in front of the scintillation counter to stop the alpha particles was attempted, but it was found that not all the alpha particles were stopped, and it was difficult to find how many did penetrate. For this part of the experiment, α^{++}/S was found from the following expression:

$$\alpha^{++}/S = C_1 - C_0 \qquad (36)$$

where C_1 and C_0 are the total counts, and the counts where the spectrometer was set at too high an energy to pass any alpha particles from the reaction, respectively. Profiles of the particles were taken at bombarding energies of 740, 863, 987, and 1114 kev, and are shown in Figure 6. The particles appearing with energies higher than the alpha particles from the reaction are both singly charged alpha particles produced in deep layers

of the target and having about one-quarter of the energy of the alpha particles being studied and protons scattered in some way through the spectrometer. It was assumed that these particles would be approximately uniformly distributed in energy, at least over a small range, so the number of them being counted would be about the same when the spectrometer was set to accept the alpha particles from the reaction as when it was set at an energy high enough to exclude them. It was further assumed that the number of "stray" particles would be a smoothly varying function of the bombarding energy, so that it would be sufficient to take four profiles and interpolate. The values of C_0 used are given in Figure 7, and it is seen that the four experimental points do lie on a smooth curve.

The results of the computations of the cross section are given in Figure 8, where the indicated probable errors are due to statistics only. There is an additional uncertainty in the scale of the ordinates of perhaps 20%, due mostly to poor data on the stopping cross sections, and partly due to uncertainty in the correction for singly charged helium nuclei.

For comparison, two points from the curve given by Burcham and Freeman[20] are also plotted in Figure 8; the agreement is considered to be satisfactory.

For the other work with alpha particle cross sections, it was necessary to know what fraction of the alpha particles would penetrate the aluminum foils before the scintillation counter with enough energy to be counted. It was also necessary to know whether any significant fraction of the protons were stopped by the foils. The latter information was found by taking

readings with and without foils of the protons scattered from oxygen in the boric anhydride target used in the work just described. It was found that about 5.3% of the protons whose energy was 1100 kev were stopped by the foils. Designating C_2 as the counts with three foils before the scintillation counter, we have the following equations:

$$C_1 = (p + \alpha^{++} + \alpha^{+})/S \tag{37}$$

$$C_2 = (0.948\ p + f\ \alpha^{++})/S \tag{38}$$

in which f designates the fraction of doubly charged alpha particles which penetrated the foil with enough energy to be counted, p is the number of protons, and it is assumed that since the singly charged alpha particles had only one-quarter as much energy as the doubly charged particles, they would all be stopped in the foils. By eliminating p from Equations 37 and 38 and solving for α^{++}/S, one gets

$$\alpha^{++}/S = (C_1 - 1.055\ C_2 - \alpha^{+}/S)/(1 - 1.055\ f) \tag{39}$$

The values of α^{+}/S were found from the profiles of Figure 6. In the region where α^{++}/S is zero,

$$\alpha^{+}/S = C_0 - 1.055\ C_0' \tag{40}$$

which may be derived from Equations 37 and 38 by noting that C_1 is replaced by C_0 and C_2 by C_0', and that α^{++}/S is zero.

By using the values of α^{++}/S given by Equation 36 for the data used in the first part of this chapter and putting them in Equation 39, f was calculated for alpha particle energies up to 1030 kev. Negative values were found for energies below 905

kev, but these are attributed to poor knowledge of α^+/S in this region, since this quantity is known only by extrapolation from higher energies. In this energy region f is probably zero. The value of f above 900 kev rose rapidly to at least 0.4, reaching this value at about 950 kev alpha particle energy. The only use made of this result was to set f equal to zero for alpha particle energies below about 900 kev, and to show that the subtraction method is untrustworthy at higher energies.

In the measurements of the cross section of $B^{10}(p\,\alpha)Be^7$ at proton energies between 1208 and 1585 kev, the targets used were thin layers of boric anhydride evaporated on 0.2 mg/cm^2 aluminum leaf. The target was oriented with the boric anhydride on the back side of the aluminum, so that both the protons and alpha particles passed through the foil. The protons scattered from the aluminum were not slowed down, but the alpha particles from the reaction and the protons scattered from the boron and the oxygen were slowed down in coming back through the foil. Since alpha particles lose energy at a much greater rate than protons, the alpha particles appeared with an energy lower than the energy of the scattered protons. The upper limit to the bombarding energy was set by the proton energy which could be obtained from the Van de Graaff; the lower limit was set by protons scattered from the boron. The energy of the scattered protons changes faster with a change in bombarding energy than does the energy of the alpha particles, so as the bombarding energy was lowered the proton energy finally became too near to the alpha particle energy, and it was no longer possible to separate the particles. There were at all bombarding energies some protons of the same

energy as the alpha particles, but it was possible to distinguish between these and the alpha particles by using the aluminum foils in front of the counter. At the alpha particle energies encountered, no alpha particles penetrated the foils with enough energy to be counted.

Three runs were made, one with one target set with θ_1 (Figure 5) equal to 28°, the other two with another target on a thinner aluminum leaf. In the latter two cases it was necessary to set the target perpendicular to the proton beam in order to achieve the same loss of energy by the alpha particles in the aluminum leaf as in the other case. Because the alpha particles exhibited considerable straggling when they emerged from the aluminum leaf, it was not possible to calculate the cross section of the reaction by Equation 23. Instead of finding the alpha particles which were produced in a lamina of the target, all of them produced in the whole target thickness were counted. The equation for the cross section, found by putting Equation 30 back in Equation 23, is now

$$\sigma(\theta) = \frac{(\alpha^{++}/S)\,S}{VC \times 6.24 \times 10^{12}} \times \frac{1}{nt} \times \frac{4\pi}{\Delta\Omega_L} \times \left(\frac{d\Omega_c}{d\Omega_L}\right)^{-1} (1 + He^{+}/He^{++}) \qquad (41)$$

α^{++}/S was calculated in the following way. The method of obtaining all the counts due to doubly charged alpha particles was in principle to take a profile of the alpha particles at one bombarding energy, and then to calculate the value of the integral

$$\alpha^{++}/S = R\int (C_1 - 1.055\, C_2)/I \; dI \qquad (42)$$

where I is the fluxmeter current and is inversely proportional

to the momentum of the alpha particles. Because in some cases the alpha particle energy varied enough at one bombarding energy to give a significant change in the correction for the alpha particles from the reaction which came from the target singly charged, the expression actually used was

$$(\alpha^{++}/S)(1 + He^{+}/He^{++}) = R \int (C_1 - 1.055\ C_2)(1 + He^{+}/He^{++})/I\ dI \tag{43}$$

The final expression for the cross section is now

$$\sigma(\theta) = (S/V\,C \times 6.24 \times 10^{12})(1/nt)(4\pi R/\Delta\Omega_L)(d\Omega_C/d\Omega_L)^{-1} \times$$
$$\times \int (C_1 - 1.055\ C_2)(1 + He^{+}/He^{++})/I\ dI \tag{44}$$

Because of the great amount of time required to take a profile of the alpha particles at each bombarding energy, this was done at only four energies: 1208, 1334, 1460, and 1585 kev. The ratio of the integral in Equation 44 to the maximum value of the integrand was found, and this ratio was used to convert from the integrand at intermediate bombarding energies to equivalent values of the integral to be used at those energies. The profiles of the alpha particles are shown in Figure 9, and the four points and the curve used for the ratio in Figure 10. The two end points were weighted more than the middle two because of the peculiar shapes of the two middle profiles. The peak at 1334 kev is flatter than normal, leading to too high a value for the ratio, and the peak at 1460 kev is narrower than normal, leading to too low a ratio. The ratio of integral to maximum value of the integrand was used for both targets although only measured for one, because the energy loss of the alpha particles

was the same for both targets and the straggling was therefore also the same.

The value of nt used in Equation 44 was found from elastic scattering of protons from the boron atoms, taking a profile of the scattered protons and integrating. Then Equation 44 applies with nt as the unknown, He^{+}/He^{++} set equal to zero, and C_2 also set equal to zero, since the scattering was done at an energy where no alpha particles were counted. It was necessary to do the proton scattering with the target in the same position as when the alpha particles were being counted, for if the boric anhydride was on the front, protons would be scattered from the thin layer of carbon on the back and emerge from the front of the target with the same energy as protons scattered from the boron on the front. The cross section of proton scattering can not be calculated from the Rutherford formula because the proton scattering is anomalous in this energy region. Since it is clear even from the raw data of the cross sections of $B^{10}(p\ \alpha)Be^{7}$ and $B^{10}(p\ \alpha)Be^{7*}$ that at least one resonance occurs near this bombarding energy, an anomaly in the proton scattering is to be expected. The proton scattering cross section was measured using a pure boron target; this work will be described in Part VI of this thesis.

The two targets were found to be nearly the same thickness: 4.10×10^{17} boron atoms per square centimeter for the first and 4.20×10^{17} boron atoms per square centimeter for the second. The value used was 4.18×10^{17}, because most of the data was taken on the second target. The uncertainty was probably larger than the difference, so using two values would not have been

worth while.

It was also necessary to correct the bombarding energy for the energy lost by the protons in passing through the aluminum foil. Combining Equations 35 and 28 and replacing the lamina in the earlier consideration by the aluminum leaf, we have

$$E_{1L} = E_{1B} - (\epsilon_1/\epsilon_{eff})(E_{2B} - E_{20}) \qquad (45)$$

where E_{1L} is the proton energy at the point where the reaction takes place and corresponds to E_1', E_{1B} is the proton energy at the front and corresponds to E_1, E_{2B} is the energy which the product particles would have if the reaction took place at the front of the leaf and corresponds to E_2, and E_{20} corresponds to E_2'' and is the energy which the actual product particles have when they leave the leaf.

The cross sections calculated for $B^{10}(p\ \alpha)Be^7$ for proton energies between 1208 and 1585 kev are plotted in Figure 8. The indicated uncertainties are those due to statistics in the counts for the particular point; there is an additional uncertainty in the scale of about 20%, due principally to poor knowledge of the stopping cross section of boron, on which nt depends, to uncertainty in the ratio of the integral in Equation 44 to the maximum value of the integrand, and to uncertainty in the factor $(1 + He^+/He^{++})$.

PART V - THE CROSS SECTION OF $B^{10}(p\ \alpha)Be^{7*}$

Some difficulty was experienced in getting the cross section for $B^{10}(p\ \alpha)Be^{7*}$. The target used for the excitation curve was a thin target of boron evaporated on aluminum leaf. It was

necessary that the target be thin in order to keep alpha particles from the reaction to the ground state from interfering with the observations. Such particles, if the reaction took place somewhat below the surface of the target, would appear at the surface of the target with energy equal to that of the particles from the reaction to the excited state. The boron target was used because the reaction is not very prolific and it was desired to increase the yield to obtain better statistics. At all bombarding energies, these alpha particles have lower energies than the protons scattered from the target and from the backing foil, so the protons from the tail of the elastic scattering curve appear as a background to the alpha particles. The target was deposited on a thin foil to avoid having elastically scattered protons from deep in the foil appear at the surface of the target with the same energy as the alpha particles which were being counted. As was described in Part II, the boron target turned out to be quite impure, and gave no better yield than boric anhydride would have done. In addition, the composition of the target had to be determined.

The target used was thick enough so that the alpha particles from the reaction did fill the spectrometer window. The expression used for the cross section was Equation 23, with α^{++}/S equal to $C_1 - 1.055C_2$:

$$\sigma(\theta) = (C_1 - 1.055C_2)(S/V\,C \times 6.24 \times 10^{12})(\epsilon_{eff}/2E_{20}) \times$$

$$\times (4\pi R/\Delta\Omega_L)(d\Omega_C/d\Omega_L)^{-1}(1 + He^+/He^{++}) \qquad (46)$$

Where the energy of the alpha particles was low enough so that

none of them penetrated the aluminum foils in front of the counter, the above expression is clearly proper. However, at proton energies above 1488 kev, the alpha particles are counted through the foils. For the final calculations, C_2 was taken equal to 6.5 at proton energies above 1488 kev. Figure 11 shows the data for this excitation curve; the extrapolated C_2 curve is shown dotted. This extrapolation is quite uncertain at the high-energy end of the curve, so the calculated cross section may be too low relative to the rest of the curve by as much as 20%.

The composition of the target was determined by comparing the yield of this target with that of two others, both of boric anhydride, on one of which three determinations were made. All of these measurements were made at a bombarding energy of about 1486 kev. Since the boric anhydride evaporates at a few hundred degrees centigrade, presumably little of the pump oil is decomposed in the process and the target is fairly pure. The ϵ_{eff} of the impure boron target could be found at one energy from Equation 46, considering the cross section as known from the measurements on the boric anhydride targets. The impurities in the boron target were principally carbon and oxygen, according to the evidence from the scattering of protons. The ratio between the stopping cross section of carbon or oxygen and that of boron for protons and alpha particles in this energy range is not constant, so it was necessary to determine the actual composition of the target. However, the stopping cross section of oxygen is very nearly proportional to that of carbon, and it was

therefore possible to consider the target as being made up of boron plus an equivalent concentration of carbon. The ratio of equivalent carbon concentration to boron concentration was then found from Equation 31. When the calculations were made, α^{++}/S was found from the expression

$$\alpha^{++}/S = (C_1 - 1.055C_2)/(1 - 1.055f) \qquad (47)$$

This is not very good, because of the uncertainty of f for alpha particles having over 900 kev energy, but since f was the same for all determinations and only the ratio is used, the result should not be greatly affected. However, f varies rapidly with E_{20} in this region, so small uncertainties in E_{20} cause large uncertainties in f and the determination of the impurity concentration is probably uncertain because of this. The final result was

$$n_C/n_B = 1.51 \pm 0.22 \qquad (48)$$

Using this result and Equation 31, the effective stopping power of the target for the reaction $B^{10}(p\ \alpha)Be^{7*}$ was computed for the whole range of bombarding energies used. The uncertainty in the composition leads to an uncertainty in ϵ_{eff} of about 9%.

The curve for the cross section is shown in Figure 8. The errors indicated are statistical; in addition there are the target composition and the usual uncertainty in ϵ_{eff}, making the scale uncertain by about 20%. It was remarked earlier that the high energy end of the curve may be too low with respect to the rest.

The gamma radiation from the Be^{7*} nuclei decaying to the ground state was also observed. Lauritsen and Thomas[11] had

previously determined that the energy of the gamma radiation from proton bombardment of B^{10} was 429 kev. The counter was at 90° to the incident proton beam and its axis was two and seven-eighths inches from the target. The target was a thin layer of boric anhydride evaporated on copper. The layer of target material had to be thin in order to avoid integrating the excitation function, there being no way of distinguishing between the gamma rays coming from different layers of the target. The target was deposited on copper in order to avoid the gamma rays from aluminum, which show resonances in this energy region. It is necessary to make a correction for the gamma radiation produced in the copper by proton bombardment, but this yield is a smooth function of bombarding energy, and the radiation is not strong.

The expression for the cross section is

$$\sigma(\theta) = (C_1 - C_B - C_{Cu})(S/V\ C \times 6.24 \times 10^{12})(1/nt\ \varepsilon)(1 - L_\gamma)^{-1} \times$$

$$\times\ (\Delta\Omega/4\pi)^{-1} \qquad (49)$$

where C_1 is the number of gamma counts on the mechanical register during proton bombardment of the target, C_B is the number of background counts to be expected during the bombardment time, C_{Cu} is the number of counts to be expected from the

proton bombardment of the copper, ε is the counter efficiency for 0.43 Mev gamma radiation, L_γ is the fraction of the gamma radiation lost through the Compton effect in the material between the target and the counter, and $\Delta\Omega/4\pi$ is the fraction of the sphere surrounding the target which is subtended by the counter.

The factor $\Delta\Omega/4\pi$ was calculated in two ways. Gamma rays of one-half million electron volts are detected mostly by the Compton electrons; these electrons are so much scattered that they enter the counter from all directions. There are two expressions available for making the calculation under these circumstances, the one given by Fowler, Lauritsen, and Lauritsen [24] and the one given by Norling[35]. The first is

$$\Delta\Omega/4\pi = (4\rho\ell/4\pi R^2)\left[1 - (\ell^2/3R^2)(1 + 3\rho/2\ell)(1 + \rho/2\ell)^{-1} + \right.$$
$$\left. + (\rho^2/R^2)(1 + \rho/4\ell)(1 + \rho/2\ell)^{-1}\right] \qquad (50)$$

where ρ is the counter radius, ℓ is one-half the effective length of the counter, and R is the distance from the source

of gamma rays to the axis of the counter. Norling's formula is

$$\Psi = \Delta\Omega / 4\pi$$

$$= (R_1/\pi\, b) F \left[(b^2 - c^2)^{\frac{1}{2}}/b,\ \text{arc tan}\ (\ell/2c) \right] \qquad (51)$$

where R_1 is the inner radius of the counter, a is the distance from the source of gamma rays to the axis of the counter, b is $a + R_1$, c is $a - R_1$, ℓ is the full effective length of the counter, and F is an elliptic integral. Each of these expressions assumes that the source is opposite the midpoint of the counter, as it was in this experiment. The two formulas give, for the geometry of this experiment, $\Delta\Omega/4\pi$ equal to 0.0315 and 0.0316, respectively.

The loss of gamma radiation in the material between the target and the counter was due to energy transferred to Compton recoil electrons. This material included a 1/16 inch strip of copper, a 1/16 inch glass window, and 0.475 inch of aluminum. The copper strip was the target backing, and the radiation went through it at an angle of 62° from the normal. The total number of electrons per square centimeter in the path of the gamma radiation was calculated. The remaining intensity is given by the expression:

$$I/I_o = e^{-\sigma n t} = (1 - L\gamma) \qquad (52)$$

The cross section used was that for loss of energy to the electrons only, as energy transferred to the scattered photons is balanced by other photons which are scattered into the counter. The value of the cross section[26] is 1.0×10^{-25} cm^2/electron, and the value of $(1 - L\gamma)$ resulting was 0.827.

The efficiency of the counter was found from the data of Bradt, Gugelot, Huber, Medicus, Preisewerk, and Scherrer[37] on the efficiency of brass- and aluminum-walled counters. The walls of the counter were very thin, but it was surrounded by an aluminum tube whose thickness was greater than the range of the Compton recoils from 0.434 Mev gamma rays. This range[38] is less than one-half millimeter. Thus the counter acts as though it had aluminum walls. The efficiency was calculated from the value for a brass-walled counter for the annihilation radiation, the value given for the ratio of efficiency of a brass-walled counter to that of an aluminum-walled counter for the annihilation radiation, and the measured slope of the efficiency curve for an aluminum-walled counter (Reference 27, Figure 3). The value used for the efficiency of an aluminum-walled counter for 0.434 Mev gamma rays was $(1.70 \pm 0.07) \times 10^{-3}$.

The thickness of the target was found by comparing the yield from the boric anhydride target with the differentiated yield from a thick B^{10} target, made by pressing amorphous boron on a copper strip. Taking into consideration the different stopping cross sections of boron and of B_2O_3, the yield of gamma rays from a layer of pure boron equal in stopping power to the unknown thickness of the target was calculated:

$$C'_1 - C'_B = (n't'/n_B t)(C_1 - C_B - C_{Cu})$$

$$= (\epsilon_{B_2O_3}/\epsilon_B)(C_1 - C_B - C_{Cu}) \qquad (53)$$

where primes refer to the layer in the pure boron target, n_B is the concentration of boron atoms in the boric anhydride target,

and the two stopping cross sections are for protons and per boron atom. The step from the first to the second form of Equation 53 is made by the use of Equation 54, which is a statement that the stopping power of the layer of boron is equal to that of the boric anhydride target.

$$\epsilon_{B_2O_3} n_B t = n' t' \epsilon_B \qquad (54)$$

$(C_1' - C_B')$ having been found from Equation 53, the stopping power of a boron layer corresponding to that number of counts is found by noting how much change in bombarding energy causes this much change in gamma ray yield. The thickness of the boric anhydride target was found to be 14.1 kev for 1.5 Mev protons, or 1.45×10^{18} boron atoms per square centimeter.

The counts due to proton bombardment of the copper were found by measuring the gamma ray yield from proton bombardment of a copper strip. These counts were corrected for the counter background. In all cases, the measurements of background were made either just before or just after the run from which the background counts were to be subtracted. The Van de Graaff was kept at the same potential, but the proton beam was interrupted some distance from the target. This procedure guarded against changes in background due either to the Van de Graaff or to other experimental work being carried on in the laboratory. The gamma rays from copper and the background were measured at six proton energies, and the values at intermediate energies found by graphical interpolation. The background counts were at worst about 25% of the total counts, and the copper counts about the same proportion. Near the peak of the resonance, the background

was about 9% of the total and the copper about 11%. In making the subtraction of copper counts, it was necessary to take into account the 14 kev energy loss of the protons before they reached the copper when the boric anhydride target was being bombarded.

The cross section for the gamma rays from $B^{10}(p\ \alpha)Be^{7*}$ at 90^{o} to the incident beam is plotted in Figure 8. The indicated errors are only those due to statistics; uncertainty in the calculated value of the target thickness, which depends on the differentiation of a thick target curve and on the stopping cross sections of boron and oxygen for protons, makes the scale of the curve uncertain by about 20%. The uncertainty in counter efficiency is only about 4%. It is to be noted that the cross section for the gamma rays does not fall off as much beyond the peak of the resonance as the cross section for the low energy group of alpha particles. This may be entirely due to poor extrapolation to high energy of the proton counts which were subtracted from total counts to give the number of low energy alpha particles (Figure 11). Considering the uncertainty in each curve, the agreement between the cross section of the gamma radiation and that of the low energy alpha particles is satisfactory.

PART VI - THE CROSS SECTION FOR PROTON SCATTERING FROM B^{10}

Measurement of the cross section of elastic scattering of protons from boron was done using a thick target of boron, made by pressing amorphous boron on a copper strip. The target was made of pure boron in order to improve statistics and to get a target whose composition was known. There was no reason for making the target thin, as the magnetic spectrometer selected the protons scattered in a thin lamina of the target. By making the target very thick, the protons would not go through to the copper backing and back through the target, and the only problem would be alpha particles from the reactions $B^{10}(p\ \alpha)Be^{7}$, Be^{7*} taking place beneath the surface of the target. The reaction to the excited state is very weak except at bombarding energies where the alpha particle energy is less than the scattered proton energy, but there is another reason for disregarding the alpha particle counts which applies to both groups. The counts resulting from any reaction are proportional to the cross section divided by the effective stopping cross section for the reaction. Equation 28 shows that the thickness of the lamina from which particles may enter the spectrometer to be counted is inversely proportional to ϵ_{eff}. Since ϵ_{eff} is about 8×10^{-18} kev cm^2/atom for proton scattering and about 40×10^{-18} kev cm^2/atom for the alpha particle reactions, the counts due to alpha particles would be only 20% of those due to protons if the cross sections were the same. But the proton scattering cross section is at least four times the others, so the counts from

alpha particles will not be more than about 5% of those from protons. Since the alpha particle cross sections do not change very rapidly with proton energy, it is possible to subtract out the alpha particle counts by measuring them with the spectrometer set for an energy higher than that of the protons.

The expression for the cross section used in this case is:

$$\sigma(\theta) = (C_1 - C_0)(S/V\ C \times 6.24 \times 10^{12})(\epsilon_{eff}/2E_{20}) \times$$

$$\times (4\pi R/\Delta\Omega_L)(d\Omega_C/d\Omega_L)^{-1} \qquad (55)$$

in which all the quantities have the meanings previously used. C_0 includes the alpha particles from inside the target. The curve of C_0 against bombarding energy was determined from points found at proton energies of 868, 992, 1116, 1240, and 1612 kev: the scattering actually took place at energies a little less than this, because the lamina selected was always a little inside the target.

The cross section is plotted in Figure 8, for comparison with the others, and in Figure 12 where the ratio to Rutherford scattering is also shown. The indicated errors are statistical only; there is an uncertainty in the scale due principally to ϵ_{eff} amounting to perhaps 10%. There is a strong anomaly in the neighborhood of the resonances in $B^{10}(p\ \alpha)Be^7$ and $B^{10}(p\ \alpha)Be^{7*}$ at 1.5 Mev, and a weak resonance at about 1.15 Mev, near the strong resonance in $B^{10}(p\ \alpha)Be^7$. The curve which shows the ratio of the observed cross section to Rutherford scattering indicates that the upper anomaly extends to the lowest energies at which we bombarded.

PART VII - OTHER ENERGY LEVELS OF Be^7

When Grosskreutz and Mather[15][16] reported the existence of a state at about 470 kev they also reported two additional excited states of Be^7, one at 205 ± 70 kev and one at 745 ± 70 kev above the ground state. Previously Mandeville, Swann, and Snowdon[29], working with the $Li^6(d\ n)Be^7$ reaction and observing the recoil protons in a photographic plate at 90° to the incident proton beam, had concluded that no state between 0.5 and 1.0 Mev was excited by as much as 10% of the disintegrations. After Grosskreutz and Mather announced their results, the levels were looked for by others. The published curves of Johnson, Laubenstein, and Richards[14] indicate the absence of levels at 205 and 745 kev. Hamermesh and Hummel[17], observing the neutrons from $Li^7(p\ n)Be^7$ with photographic plates, found no tracks corresponding to either of the states at 205 and 745 kev which could not be attributed to background. Van Patter, Sperduto, and Buechner[21], studying the alpha particles from $B^{10}(p\ \alpha)Be^7$, found at a proton energy of 1.6 Mev no sign of an alpha particle group corresponding to the 205-kev state, and they stated that at 1.79 Mev bombarding energy the group corresponding to the 745-kev state was not excited in more than 1% as many cases as the group leaving the Be^7 in the ground state.

A search was made for alpha particles from $B^{10}(p\ \alpha)Be^{7*}$ leaving the Be^7 nucleus excited by approximately 200 kev. The target was the same as that used for the two runs of the cross section of $B^{10}(p\ \alpha)Be^7$ in the higher bombarding energy region, a thin layer of boric anhydride on the back side of an aluminum leaf. The proton energy was 1.46 Mev at the boric anhydride

layer. The data obtained are shown in Figure 13, where the indicated errors are those due to statistics. For alpha particles of the energy of these, the three foils in front of the counter were enough to stop them all. The energies at which the two groups of alpha particles appeared agree with the energies calculated from the foil thickness. The conclusion to be drawn from these data is that at a proton energy of 1.46 Mev, no state in Be^7 near 300 kev is excited as much as one-tenth as often as either the ground state or the state at 434 kev. Excitation of the state at 745 kev was not attempted, since if the state exists the barrier penetration factor for the alpha particles would be so low that the reaction could not have been observed at the proton energies available. It must be pointed out that Grosskreutz and Mather used proton energies of 5.1 Mev, while no one else has bombarded at over 4 Mev. It is possible that the states are excited only at large proton energy.

Bashkin, Ajzenberg, Browne, Goldhaber, Laubenstein, and Richards[30] observed a resonance in $Li^6(p\ \alpha)He^3$ at 1.9 Mev proton energy and in the elastic scattering of protons from Li^6 at 1.9 Mev. From this they conclude that an excited state exists in Be^7 at 7.1 Mev.

PART VIII - CONCLUSIONS

From the work described in Chapters 3 and 7 it is concluded that there exists in Be^7 an excited state 434 $\pm$ 5 kev above the ground state, that the evidence for states in the neighborhood of 300 and of 750 kev must be regarded as quite doubtful, and that a state probably exists at about 7.1 Mev above the ground state. The Q-value of $B^{10}(p\ \alpha)Be^7$ is 1.148 $\pm$ .006 Mev and of

$B^{10}(p\ \alpha)Be^{7*}$ is 0.714 ± .006 Mev.

Referring to Equations 12 and 15, numbers can now be substituted for some of the quantities. Q_2 is given by Tollestrup, Fowler, and Lauritsen[31] as 2.791 Mev, and $E_x(Li^{7*})$ is 0.478 Mev. Equation 12 then gives 3.80 x 10^{12} cm^{-1} for $\overline{(1/r)}$, and Equation 15 gives for the first excited state 3.70 x 10^{12} cm^{-1} for $\overline{(1/r^*)}$, a decrease of 2.5%, corresponding to an increase of 2.5% in the average distance between protons when the nuclei go to the excited state. These results are independent of any nuclear model. If one makes the very general assumption that the nucleus expands uniformly, then the nuclear radius increases by 2.5%. This is a reasonable result, for the addition of energy to the nucleus should result in work being done against the nuclear forces which attract the nucleons. If some particular charge distribution in the nucleus is assumed, then $\overline{(1/r)}$ can be calculated in terms of the nuclear dimensions, by the expression

$$\overline{(1/r)} = (1/Z^2) \int\int (\rho_1\rho_2/r)\ d\tau_1 d\tau_2 \qquad (56)$$

where ρ_1 and ρ_2 are the probability densities for protons, and $d\tau_1 d\tau_2$ are the elements of volume. In particular, the value of $\overline{(1/r)}$ corresponding to a uniform distribution of protons throughout a solid sphere is 6/5R, and that corresponding to a uniform distribution over a spherical shell is 1/R, where R is in each case the radius of the sphere. From the results given above, R may be calculated in these cases:

	R	R*
Solid sphere	3.16 x 10^{-13} cm	3.24 x 10^{-13} cm
Spherical shell	2.63 x 10^{-13} cm	2.70 x 10^{-13} cm

The usual expression for R, $e^2A^{1/3}/2mc^2$, gives for nuclei of mass 7 a radius of 2.70×10^{-13} cm. This does not indicate that these nuclei actually are spherical shells, but it is believed to be significant that the energy difference between the ground states of the nuclei can be accounted for by electrostatic repulsion on the basis of a reasonable charge distribution and a radius which agrees with indications from other types of experiments. It is further believed to be significant that there exists an excited state of Be^7 whose excitation energy is nearly that of the well known state in Li^7, and that the energy difference between these states can also be accounted for as electrostatic repulsion. The existence of the state with nearly the same excitation energy is in agreement with predictions made on the basis of equality of proton-proton and neutron-neutron forces. That the average distance between protons is increased and that the increase is slight are in agreement with the picture of addition of excitation energy resulting in work being done against the nuclear forces, and in agreement with the comparison of the excitation energy with the binding energy.

The existence of the state at 7.1 Mev in Be^7 does not at present give much information about the equality of proton-proton and neutron-neutron forces. This state may not correspond to the 7.38 Mev state in Li^7. It is true that a level in Be^7 should have less excitation energy than the level in Li^7 to which it corresponds, because there is more decrease of Coulomb energy in Be^7 than in Li^7 for any given nuclear expansion. At this high excitation, however, it is to be expected that several excited states might exist, and in fact Bashkin et al.[30] found

indications of another state somewhat lower. It is not clear that several states do not exist in Li^7 in this region. Even if it should be true that the known states in Be^7 and Li^7 do correspond, it would be difficult to make any quantitative calculations, because both of these states are unstable to heavy-particle emission. This situation has been worked out for states in C^{13} and N^{13} by Mr. R. G. Thomas[32], and is complicated by the fact that there is a large probability of finding the particles which can be emitted in the potential barrier, and the charge distribution is almost certainly radically changed from the ground state.

By analyzing the cross sections of the various reactions at the two resonances (Figure 8) one can obtain an indication of the nature of the states of the compound nucleus C^{11} which are formed in the reactions. The procedure followed was to assume a spin and parity for the level of the compound nucleus, and then to see whether that assumption agreed with the experimental evidence. Assumption of a spin value permits the calculation of the partial widths due to protons and alpha particles from the Breit-Wigner formula

$$\sigma_{12}(\theta) = 4\pi\lambda^2 (2J + 1)\Gamma_1\Gamma_2/(2S + 1)(2i + 1)\Gamma^2 \qquad (57)$$

and from the assumption that no other process competes strongly with re-emission of the protons and with emission of one group of alpha particles.

$$\Gamma = \Gamma_1 + \Gamma_2 \qquad (58)$$

It is further assumed that only one resonance affects the

observations strongly at any given bombarding energy, so the Breit-Wigner formula applies. Since the cross section, the spins of the bombarding particle and target nucleus, and the total width Γ are known, Equations 57 and 58 are enough to determine Γ_1 and Γ_2. However, the two equations are symmetric in the two unknowns, and it is necessary to use some other criterion for distinguishing which solution of the equations is to be associated with each Γ. In the case of the two resonances being studied, it was known that at the lower resonance, Γ_α was larger than Γ_p, while at the other, Γ_p was larger than Γ_α. This relation comes from applying the Breit-Wigner formula both to $B^{10}(p\ \alpha)Be^7$ or $B^{10}(p\ \alpha)Be^{7*}$ and to $B^{10}(p\ p)B^{10}$, obtaining

$$\frac{\Gamma_p}{\Gamma_\alpha} = \frac{\sigma_{pp}}{\sigma_{p\alpha}} \tag{59}$$

The first test of the choice of the spin is a reasonable value for the ratio of the partial widths.

A second test of the assumption of the spin and parity of the intermediate nucleus is the relative values of the partial widths of the two groups of alpha particles. The ratio of the partial widths may be predicted roughly from the spin and parity of the compound nucleus, and compared with the experimental ratio of cross sections. For a given spin and parity of the compound nucleus, the angular momentum carried off by the emitted particle is limited to only a few values by conservation of spin and parity. The ground state of Be^7 was taken to be spin 3/2 and odd parity, and the excited state spin 1/2 and odd parity, in order that the states correspond with the two

lowest states of Li^7. For each assumption of a spin and parity of C^{11}, the angular momentum of the incoming or outgoing particle wave is shown in Table 3.

TABLE 3

C^{11} Spin	C^{11} Parity	Proton Wave	Alpha Particle Waves	
			Main Group	Low Energy Group
1/2	Even	D	P	P
1/2	Odd	F	D	S
3/2	Even	D	P	P
3/2	Odd	P	S	D
5/2	Even	S	P	F
5/2	Odd	P	D	D
7/2	Even	S	F	F
7/2	Odd	P	D	G

In the table only the wave of lowest possible angular momentum is shown for each transition, because the barrier penetrability will make this one dominate the others in the cases where more than one is possible.

When the partial wave responsible for the reaction has been determined, it is possible to make an estimate of the ratio of the partial widths of the two groups of alpha particles. The partial width may be expressed as follows:(33)

$$\Gamma_p = PE^2G \qquad (60)$$

where P is defined as the ratio of the wave function of the emitted particle integrated over a sphere of large radius to

its wave function integrated over the surface of the nucleus, E is the total kinetic energy in center of mass coordinates, and G is the intrinsic width. It was assumed that G was approximately the same for the two alpha particle groups at a given resonance; then the ratio of the cross sections would be given by the ratio of the quantities $(PE^{\frac{1}{2}})$ for the two groups of particles. The values of this factor for protons and alpha particles taking part in the reactions at the two resonances were found from the curves of Christy and Latter[33] and from the equations given by Bethe[34]. The expressions used were Equations 629, 631 and 600a, except than in the latter the nuclear radius was taken to be $e^2 A^{1/3}/2mc^2$. The results of the calculations are given in Table 4. The actual expression used with the formulas of Bethe was

$$PE^{\frac{1}{2}}(M/M_p)^{-\frac{1}{2}} = E_B^{\frac{1}{2}}(M/M_p)^{-\frac{1}{2}}\, e^{-2C} \qquad (61)$$

This gives the same normalization as the expression of Christy and Latter.

TABLE 4

Nuclear Penetration Factors for $B^{10}(p\ \alpha)Be^{7}$, Be^{7*} and $B^{10}(p\ p)B^{10}$

Protons	Alpha Particles	
	Main Group	Low Energy Group
Resonance at 1.10 Mev Proton Energy		
S-wave .40	.52	.26
P-wave .13	.23	.091
D-wave .011	.042	.0154
Resonance at 1.52 Mev Proton Energy		
S-wave .62	.74	.49
P-wave .26	.37	.20
D-wave .032	.086	.038
F-wave	.0101	.0036

Considering first the resonance at 1.10 Mev, one sees that the cross section for the main group of alpha particles is much larger than that for the low energy group, being about 0.14 barn in comparison to probably not more than 0.01 barn. It is clear that at this resonance, a state of C^{11} must be chosen such that the low energy group of alpha particles must be emitted with more angular momentum than the main group, for the ratio of PE^2 for the two groups when the angular momentum is the same is never more than three. Examples of such states of C^{11} are 3/2 odd, 5/2 even, and 7/2 odd. All the rest on the list are eliminated by this test. States of higher angular momentum than

those listed require such high angular momentum incoming and outgoing particles that the reaction would be very improbable.

The third test of the assumed values of the spin and parity of the state of the compound nucleus is that the values obtained for G should be reasonable. The intrinsic widths of nuclear states are rarely more than 1 Mev, and then only in some special case, such as the state of N^{13} associated with proton bombardment of C^{12}.

At the lower resonance, the second test of spin and parity assumptions was applied first, and the three possibilities left were 3/2 odd, 5/2 even, and 7/2 odd. Next the first test was applied, and last the third test. The results were as follows:

TABLE 5

States of C^{11}	Γ_p	Γ_α	Γ_p/Γ_α	σ_{pp}	G_p	G_α
3/2 Odd	.107 Mev	.393 Mev	.272	.038 barn	.82 Mev	.76 Mev
5/2 Even	.065 Mev	.435 Mev	.149	.021 barn	.16 Mev	1.9 Mev
7/2 Odd	.047 Mev	.453 Mev	.104	.015 barn	.36 Mev	4.1 Mev

Since the proton scattering cross section exhibits only a small rise on a large background, any of the assumptions of the C^{11} state would satisfy the first test, but the large values for G_α make the 5/2 even assumption very doubtful and exclude the 7/2 odd assumption.

An attempt was made to check the assignment of spin and parity by computing the proton scattering cross section by Equation 61g of Bethe's paper[34]. The formula was modified by inserting a factor $(2J + 1)/(2S + 1)(2i + 1)$ before the second term

on the right side, to account for the spins of the boron and hydrogen nuclei. The results indicated only that the proton wave must have small angular momentum to prevent a larger anomaly than the one observed.

At the higher resonance the ratio of the two alpha particle groups is reversed. The low energy group has a cross section of about 0.14 barn, while the main group has only about 0.035 attributable to a resonance at this point, and this value is very uncertain. The width of the resonance was taken as .3 Mev.

The first assumption made for the spin and parity of the C^{11} state responsible for this resonance was spin 1/2 and odd parity, since this is the only state requiring a higher angular momentum for the main group of alpha particles than for the low energy group. Solving Equations 57 and 58 for this case led to complex values of the partial widths; only changing the spin value or halving the observed low energy alpha particle cross section would make the partial widths real. That the cross section was twice the real value seemed highly improbable, but the calculations for this state and for the 1/2 even state were carried through on this basis. The next best solution to the second test of the spin and parity assignment is to have the same wave emitted for the two groups of alpha particles. Calculations were made for all the states of Table 3 for which this is true, and the results are given in the following table.

TABLE 6

States of C^{11}	Γ_p (Mev)	$\Gamma_{\alpha'}$ (Mev)	σ_{pp} (barn)	G_p (Mev)	$G_{\alpha'}$ (Mev)	G_α (Mev)
1/2 Even	.15	.15	.074	4.7	.75	0
1/2 Odd	.15	.15	.074	50	.31	0
3/2 Even	.15	.14	.15	4.7	.71	.023
5/2 Odd	.219	.065	.47	.84	1.7	.19
7/2 Even	.043	.246	.80	.40	12	1.1

In Table 6 it was assumed that the reaction to the ground state of Be^7 occurred in one-quarter as many cases as the reaction to the excited state. If it was assumed that the main group of alpha particles did not exhibit any resonance at this energy, G_α was equal to zero, but the other values were little affected. On the basis of this table, the most reasonable assignment of spin and parity to the state of C^{11} involved is spin 5/2 and odd parity.

Considering the proton scattering on the basis of this spin assignment and Bethe's Equation 619 indicates that a large rise in the cross section is to be expected, approximately accounting for the observed cross section.

APPENDIX - DERIVATION OF FORMULAS FOR CONVERTING SOLID ANGLE AND ANGLE OF OBSERVATION FROM LABORATORY TO CENTER OF MASS COORDINATES

The following derivation is non-relativistic. The formulas are designed to be used for calculations of cross sections of reactions in which none of the particles have more than a few Mev energy, so the error introduced by using classical instead of relativistic mechanics is much less than the errors of observation. The starting point of the derivation is an equation which states that the tangent of the angle between the direction of motion of the incident particle and the path of the observed particle is the ratio of the components of velocity of the observed particle perpendicular and parallel to the path of the incident particle.

$$\tan \theta_L = \sin \theta_L / \cos \theta_L = \frac{(2E_{2C}/M_2)^{\frac{1}{2}} \sin \theta_C}{(2E_{2C}/M_2) \cos \theta_C + V_{CM}} \qquad (A-1)$$

where the subscripts C and L refer to center of mass and laboratory coordinates, and V_{CM} is the velocity of the center of mass coordinate system with respect to the laboratory coordinates. Using conservation of momentum, this velocity may be expressed as follows:

$$V_{CM} = (2M_1E_{1L})^{\frac{1}{2}}/(M_1 + M_0) = (2M_1E_{1L})^{\frac{1}{2}}/M \qquad (A-2)$$

where to simplify notation, the quantity M is introduced.

$$M = M_1 + M_0 = M_2 + M_3 \qquad (A-3)$$

The last member of the equation uses an approximation sufficiently good for this derivation. The definition in center of mass coordinates of the Q-value of the reaction is

$$E_{2C} + E_{3C} = E_{1C} + E_{OC} + Q \qquad (A-4)$$

These energies are related by the momentum considerations which define the center of mass coordinate system:

$$(2M_1E_{1C})^{\frac{1}{2}} = (2M_OE_{OC})^{\frac{1}{2}} \qquad (A-5)$$

$$(2M_2E_{2C})^{\frac{1}{2}} = (2M_3E_{3C})^{\frac{1}{2}} \qquad (A-6)$$

The next step is to eliminate E_{1C} and E_{3C} from Equation A-4 by the use of Equations A-5 and A-6, to simplify by using A-3, and to substitute the value of E_{OC} in terms of M_O and V_{CM}:

$$E_{2C} = (MM_3Q + M_OM_3E_{1L})/M^2 \qquad (A-7)$$

Next the statement is made that the component of velocity of the observed particle perpendicular to the incident proton beam is the same in both systems of coordinates:

$$(2E_{2L}/M_2)^{\frac{1}{2}}\sin\theta_L = (2E_{2C}/M_2)^{\frac{1}{2}}\sin\theta_C \qquad (A-8)$$

At this time it is convenient to define a quantity β, which is the same as the γ used by Schiff[23]:

$$\beta = (M_1M_2E_{1L})^{\frac{1}{2}}/(MM_3Q + M_OM_3E_{1L})^{\frac{1}{2}} \qquad (A-9)$$

The next step is to put Equation A-1 in a more useful form by eliminating $\sin\theta_C$ in the numerator of the right side by the use of Equation A-8, by substituting for E_{2C} in the denominator of the right side its equivalent in terms of Equation A-7, to substitute for V_{CM} from Equation A-2, and to simplify using Equation A-9:

$$\cos\theta_C = \beta\, M(E_{2L}/M_1M_2E_{1L})^{\frac{1}{2}}\cos\theta_L - \beta \qquad (A-10)$$

It is now useful to eliminate E_{2L}, since the reaction is fully determined by the various masses, the Q-value, the angle of observation, and the bombarding energy. The expression used

$$E_{2L}^{\frac{1}{2}} = (M_1M_2E_{1L})^{\frac{1}{2}}\cos\theta_L/M + (QM_3/M + (M_3 - M_1)E_{1L}/M + \\ + M_1M_2E_{1L}\cos^2\theta_L/M^2)^{\frac{1}{2}} \qquad (A\text{-}11)$$

can be derived from Equation 16 by solving for $E_{2L}^{\frac{1}{2}}$. When this expression is used to replace E_{2L} in Equation (A-10), and the resulting equation is simplified by the use of Equation (A-9), the result is

$$\cos\theta_C = -\beta\sin^2\theta_L + (1 - \beta^2\sin^2\theta_L)^{\frac{1}{2}}\cos\theta_L \qquad (34)$$

In either the laboratory or the center of mass coordinates the element of solid angle is given by

$$d\Omega = \sin\theta\, d\theta\, d\phi \qquad (A\text{-}12)$$

where the angles appropriate to the coordinate system are used. But the azimuthal angle, ϕ, is the same in the two coordinate systems, so the ratio of the elements of solid angle is

$$d\Omega_C/d\Omega_L = \sin\theta_C d\theta_C/\sin\theta_L d\theta_L \qquad (A\text{-}13)$$

Equation 34 is now differentiated implicitly with respect to θ, noting that β does not depend on θ.

$$\sin\theta_C d\theta_C = 2\beta\sin\theta_L\cos\theta_L d\theta_L + (1 - \beta^2\sin^2\theta_L)^{\frac{1}{2}}\sin\theta_L d\theta_L + \\ + (1 - \beta^2\sin^2\theta_L)^{-\frac{1}{2}}\beta^2\cos^2\theta_L\sin\theta_L d\theta_L \qquad (A\text{-}14)$$

This equation may now be divided through by $\sin\theta_L d\theta_L$ and the result substituted for the right member of equation (A-13).

$$d\Omega_C/d\Omega_L = 2\beta \cos\theta_L + (1 - \beta^2 \sin^2\theta_L)^{\frac{1}{2}}$$

$$+ \beta^2 \cos^2\theta_L (1 - \beta^2 \sin^2\theta_L)^{-\frac{1}{2}} \qquad (32)$$

REFERENCES

1. Fowler, Delsasso, and Lauritsen, Phys. Rev. 49, 561 (1936).
2. Lauritsen, National Research Council Nuclear Science Series, No. 5 (1949).
3. Inglis, Phys. Rev. 78, 104 (1950).
4. Chao, Lauritsen, and Tollestrup, Phys. Rev. 76, 586 (1949).
5. Feenberg and Goerzel, Phys. Rev. 70, 597 (1946).
6. Lauritsen, Lauritsen, and Fowler, Phys. Rev. 59, 241 (1941).
7. Fowler, Lauritsen, and Lauritsen, Rev. Sci. Instr. 18, 818 (1947).
8. Rubin and Rasmussen, Phys. Rev. 78, 83 (1950).
9. C. W. Snyder, Thesis, California Institute of Technology (1948).
10. Snyder et al., to be published in the Review of Scientific Instruments.
11. Lauritsen and Thomas, Phys. Rev. 78, 88 (1950).
12. Whaling and Butler, Phys. Rev. 78, 72 (1950).
13. Gibson (Cambridge), to be published.
14. Johnson, Laubenstein, and Richards, Phys. Rev. 77, 413 (1950).
15. Grosskreutz and Mather, Phys. Rev. 77, 580 (1950).
16. Grosskreutz and Mather, Phys. Rev. 77, 767 (1950).
17. Hamermesh and Hummel, Phys. Rev. 78, 73 (1950).
18. Freier, Rosen, and Stratton, Bull. A. P. S. 25, No. 3, 48 (1950).
19. Hall, Phys. Rev. 77, 411 (1950).
20. Burcham and Freeman, Phil. Mag. 41, 337 (1950).
21. Van Patter, Sperduto, and Buechner, M. I. T. Progress Report, April 1, 1950.

22. Livingston and Bethe, Rev. Mod. Phys. 9, 245 (1937).

23. Schiff, Quantum Mechanics (McGraw-Hill Book Company, Inc., New York, 1949), p. 99, Equation (18.7).

24. Fowler, Lauritsen, and Lauritsen, Rev. Mod. Phys. 20, 236 (1948).

25. Norling, Arkiv för Matematik, Astronomi, o. Fysik 27A, No. 27 (1941).

26. Lauritsen, Am. J. Roentgenology and Radium Therapy 30, 380 (1933).

27. Bradt, Gugelot, Huber, Medicus, Preisewerk, and Scherrer, Helv. Phys. Acta 19, 77 (1946).

28. Bleuler and Zünti, Helv. Phys. Acta 19, 375 (1946).

29. Mandeville, Swann, and Snowdon, Phys. Rev. 76, 980 (1949).

30. Bashkin, Ajzenberg, Browne, Goldhaber, Laubenstein, and Richards, Bull. A. P. S. 25, No. 3, 47 (1950).

31. Tollestrup, Fowler, and Lauritsen, to be published.

32. R. G. Thomas, private communication.

33. Christy and Latter, Rev. Mod. Phys. 20, 185 (1948).

34. Bethe, Rev. Mod. Phys. 9, 69 (1937).

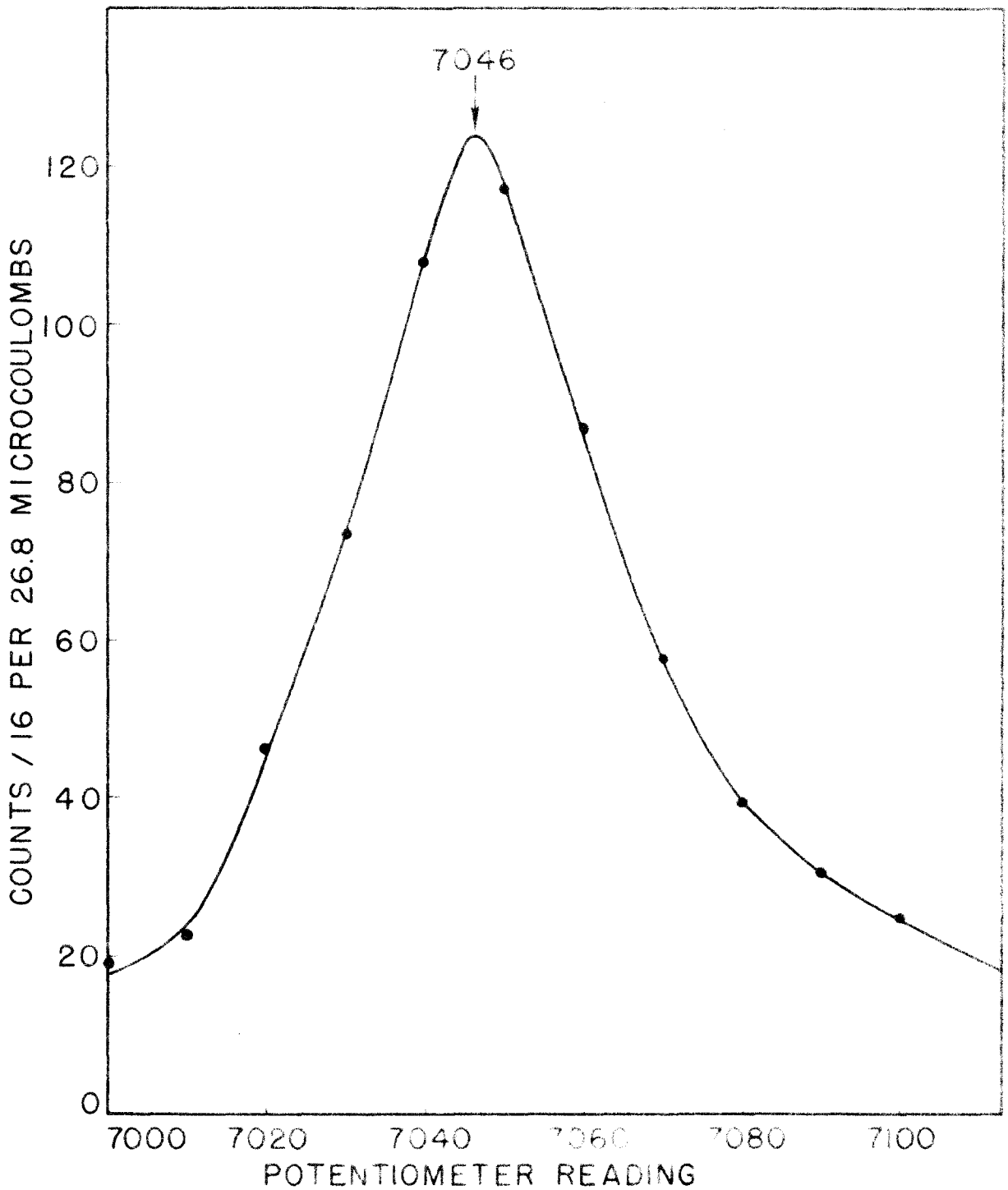

CALIBRATION OF ELECTROSTATIC ANALYZER

GAMMA RAYS FROM $F^{19} + p$ AT 873.5 KEV

FIGURE 1

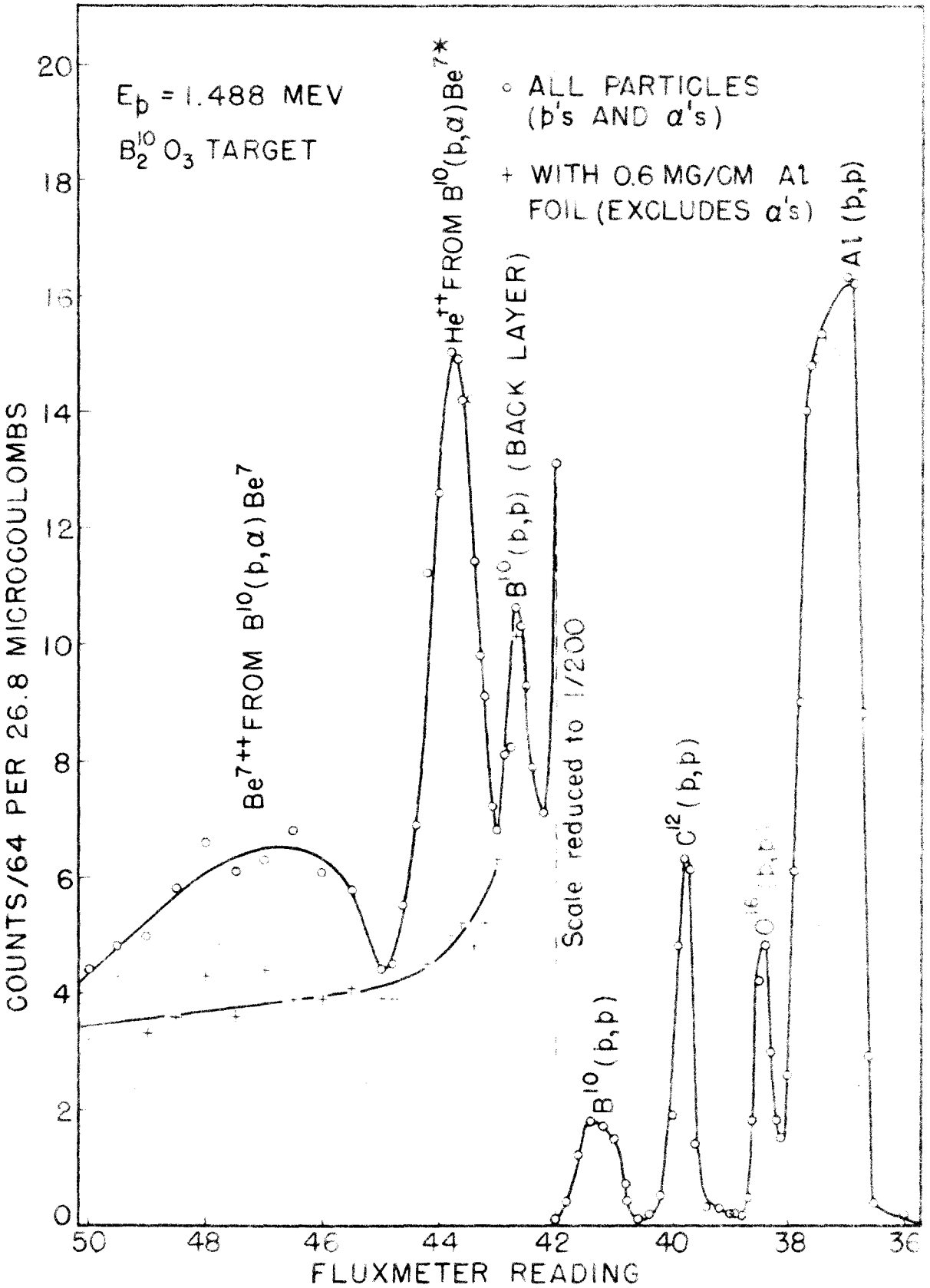
E_p = 1.488 MEV
$B_2^{10}O_3$ TARGET
○ ALL PARTICLES (p's AND α's)
+ WITH 0.6 MG/CM Al FOIL (EXCLUDES α's)
He^{++} FROM $B^{10}(p,\alpha)Be^{7*}$
Be^{7++} FROM $B^{10}(p,\alpha)Be^{7}$
$B^{10}(p,p)$ (BACK LAYER)
Scale reduced to 1/200
$B^{10}(p,p)$
$C^{12}(p,p)$
O^{16} ???
Al (p,p)
COUNTS/64 PER 26.8 MICROCOULOMBS
FLUXMETER READING
0
2
4
6
8
10
12
14
16
18
20
50
48
46
44
42
40
38
36

FIGURE 2

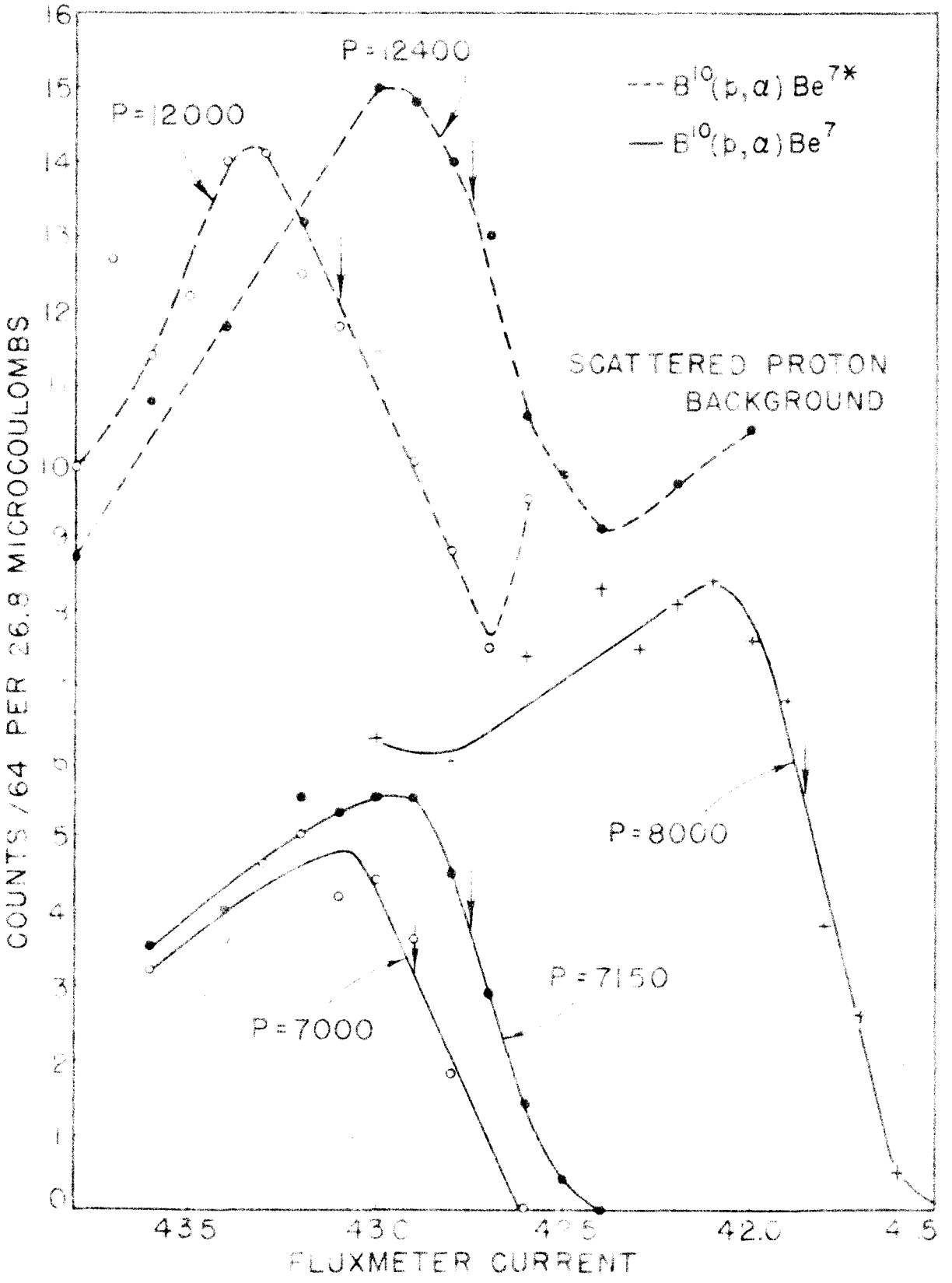

ALPHA PARTICLE PROFILES
OF $B^{10}(p,\alpha)Be^{7}, Be^{7*}$
FIGURE 3

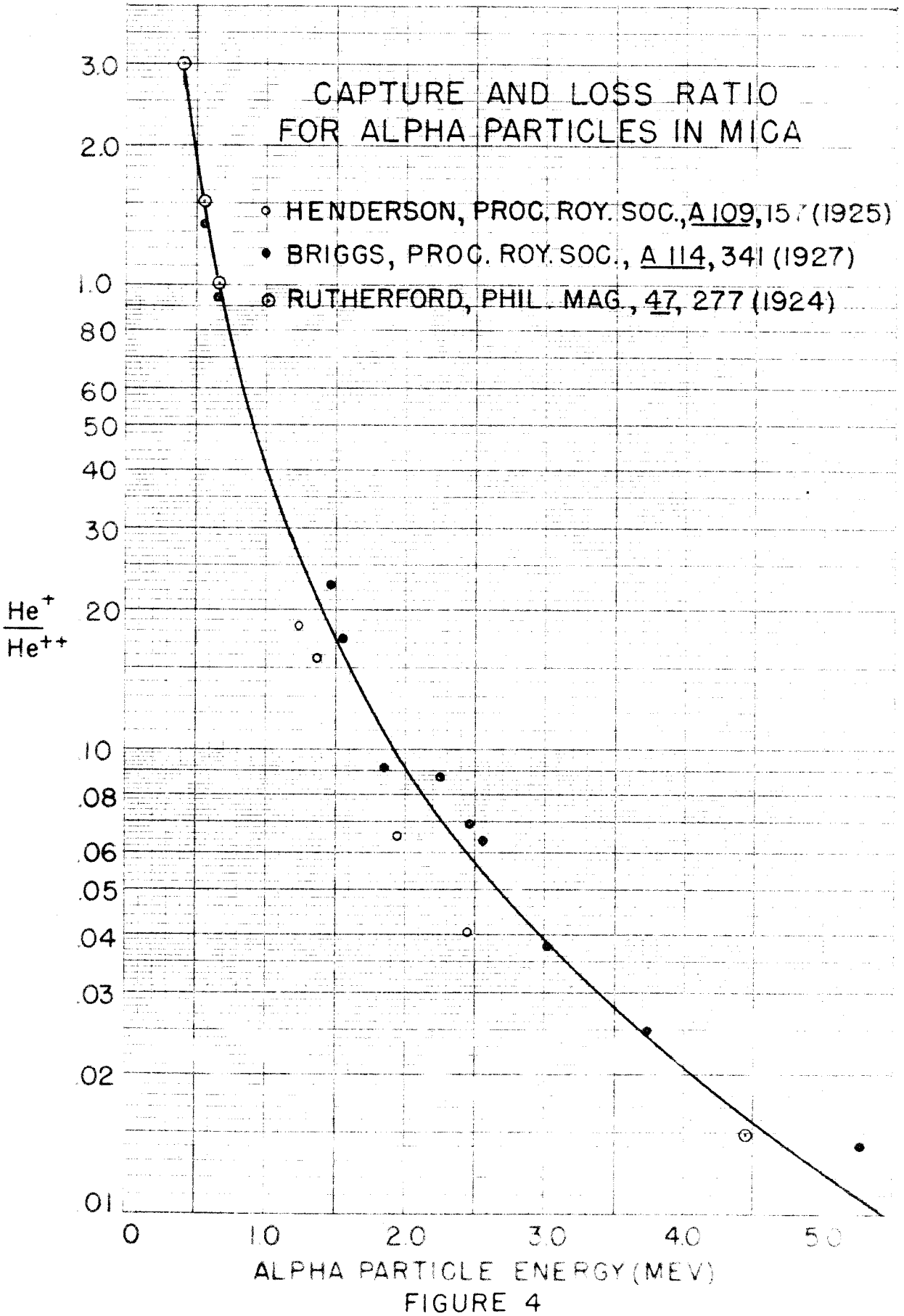
CAPTURE AND LOSS RATIO
FOR ALPHA PARTICLES IN MICA
HENDERSON, PROC. ROY. SOC., A 109, 157 (1925)
BRIGGS, PROC. ROY. SOC., A 114, 341 (1927)
RUTHERFORD, PHIL. MAG., 47, 277 (1924)
He+ / He++
3.0
2.0
1.0
80
60
50
40
30
20
10
.08
.06
.05
.04
.03
.02
.01
0
1.0
2.0
3.0
4.0
5.0
ALPHA PARTICLE ENERGY (MEV)

FIGURE 4

MAGNETIC SPECTROMETER ANALYSIS OF PARTICLES FROM THICK TARGETS

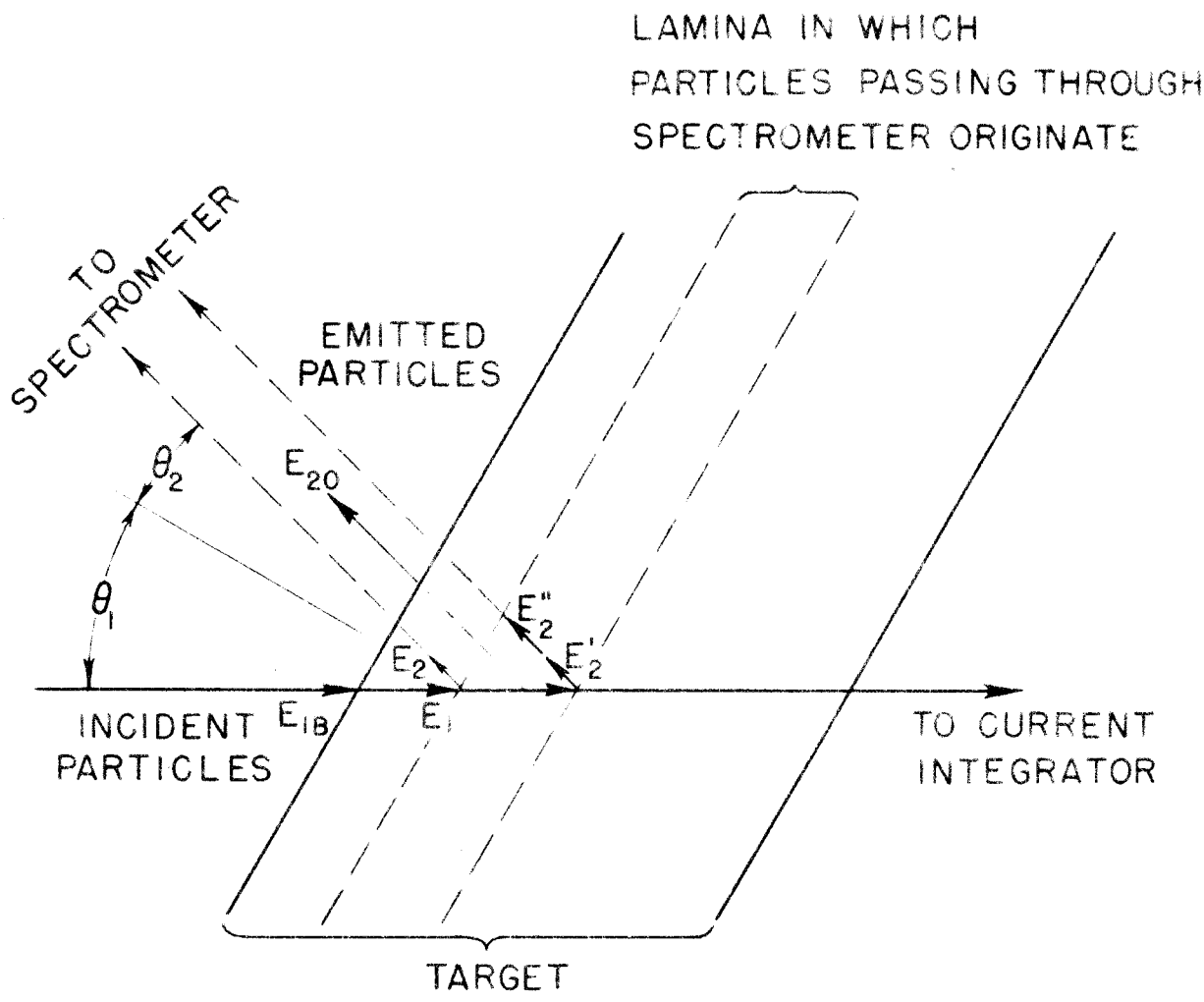

FIGURE 5

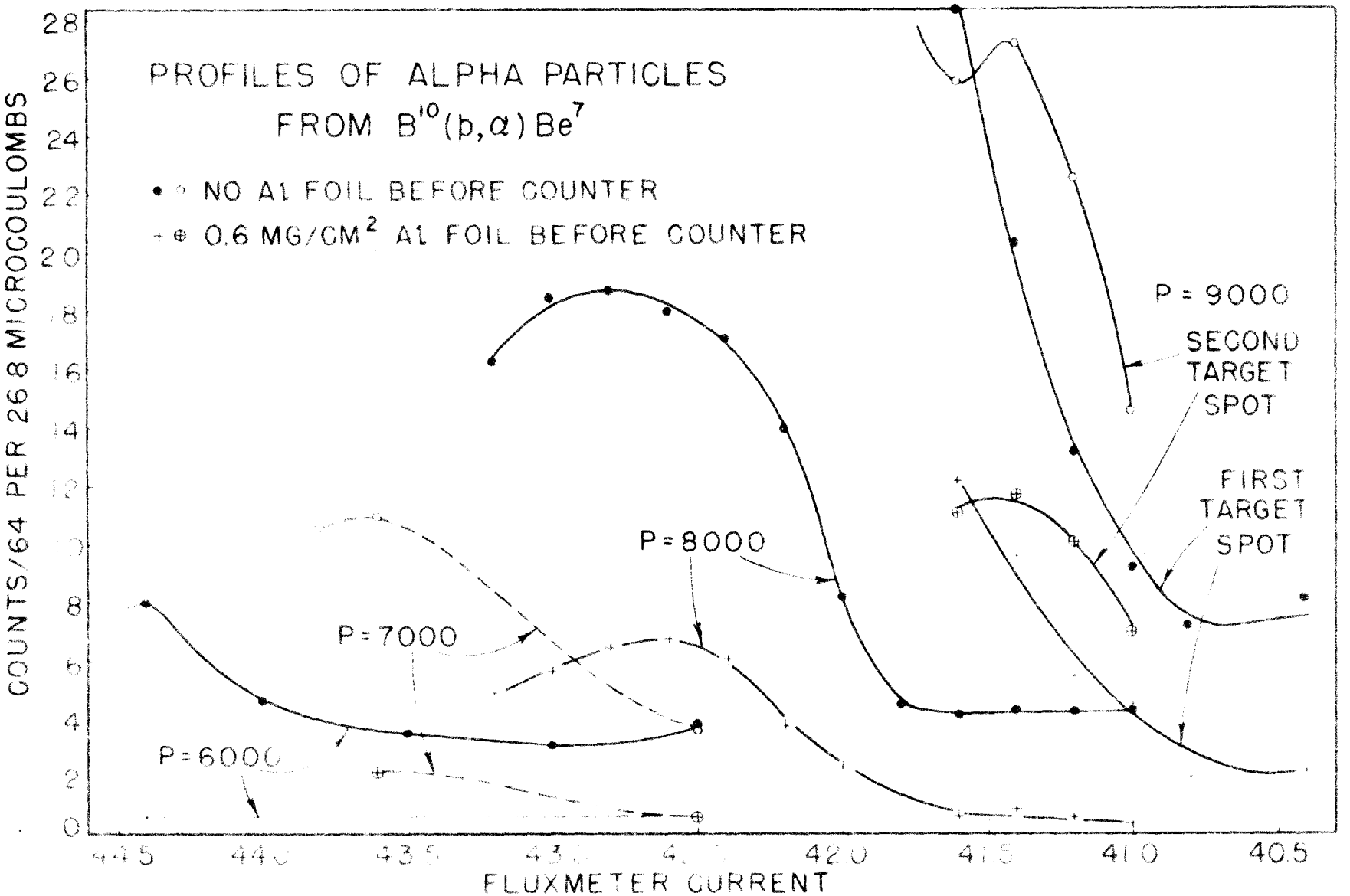
PROFILES OF ALPHA PARTICLES
FROM $B^{10}(p,\alpha)Be^7$
• ○ NO Al FOIL BEFORE COUNTER
+ ⊕ 0.6 MG/CM² Al FOIL BEFORE COUNTER
COUNTS/64 PER 2.68 MICROCOULOMBS
FLUXMETER CURRENT
P = 9000
SECOND TARGET SPOT
FIRST TARGET SPOT
P = 8000
P = 7000
P = 6000
28
26
24
22
20
18
16
14
12
10
8
6
4
2
0
44.5
44.0
43.5
43.0
42.5
42.0
41.5
41.0
40.5

FIGURE 6

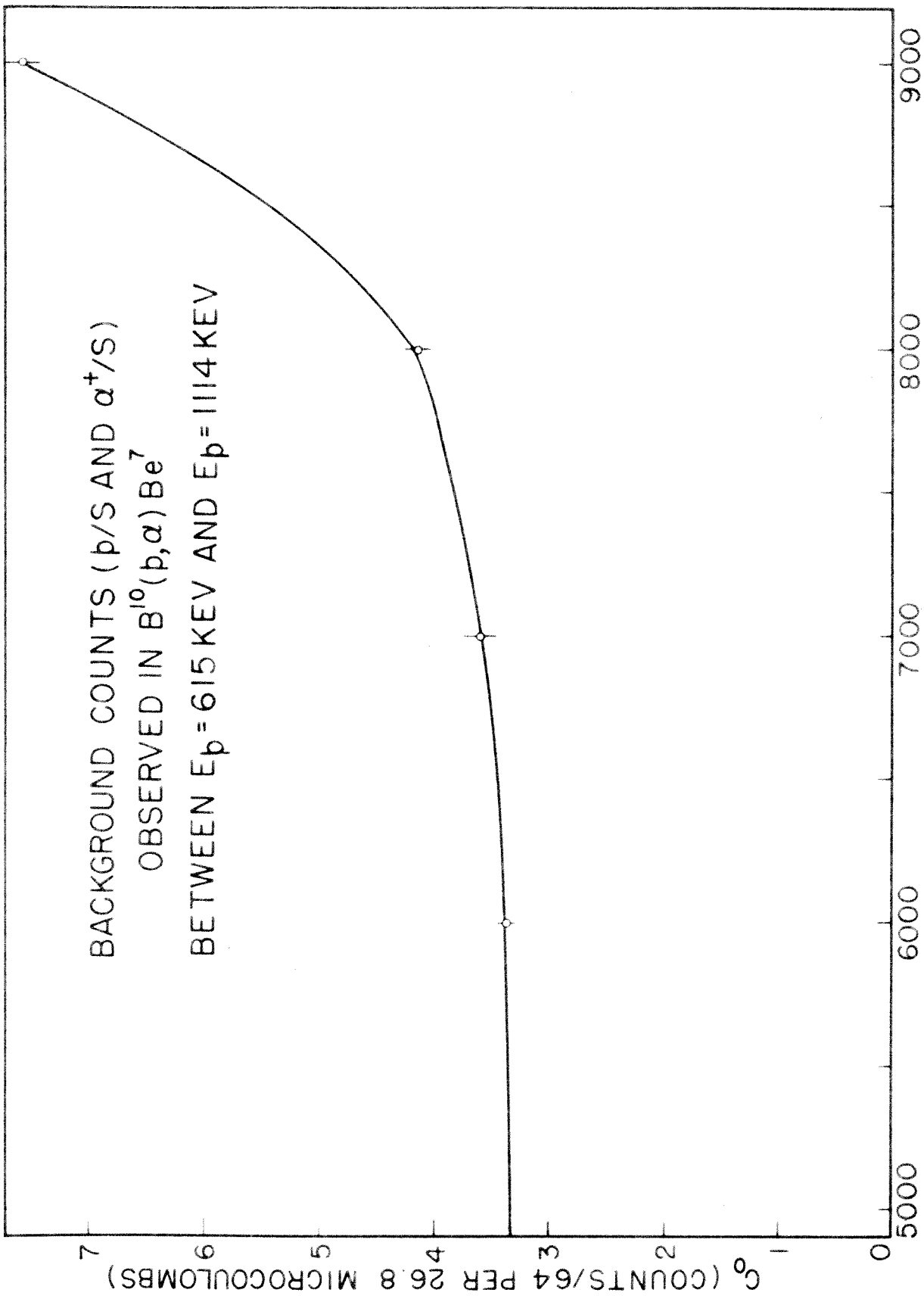
BACKGROUND COUNTS (p/S AND α^+/S)
OBSERVED IN $B^{10}(p,\alpha)Be^7$
BETWEEN E_p = 615 KEV AND E_p = 1114 KEV
C_o (COUNTS/64 PER 26.8 MICROCOULOMBS)
0
1
2
3
4
5
6
7
5000
6000
7000
8000
9000
POTENTIOMETER READING

FIGURE 7

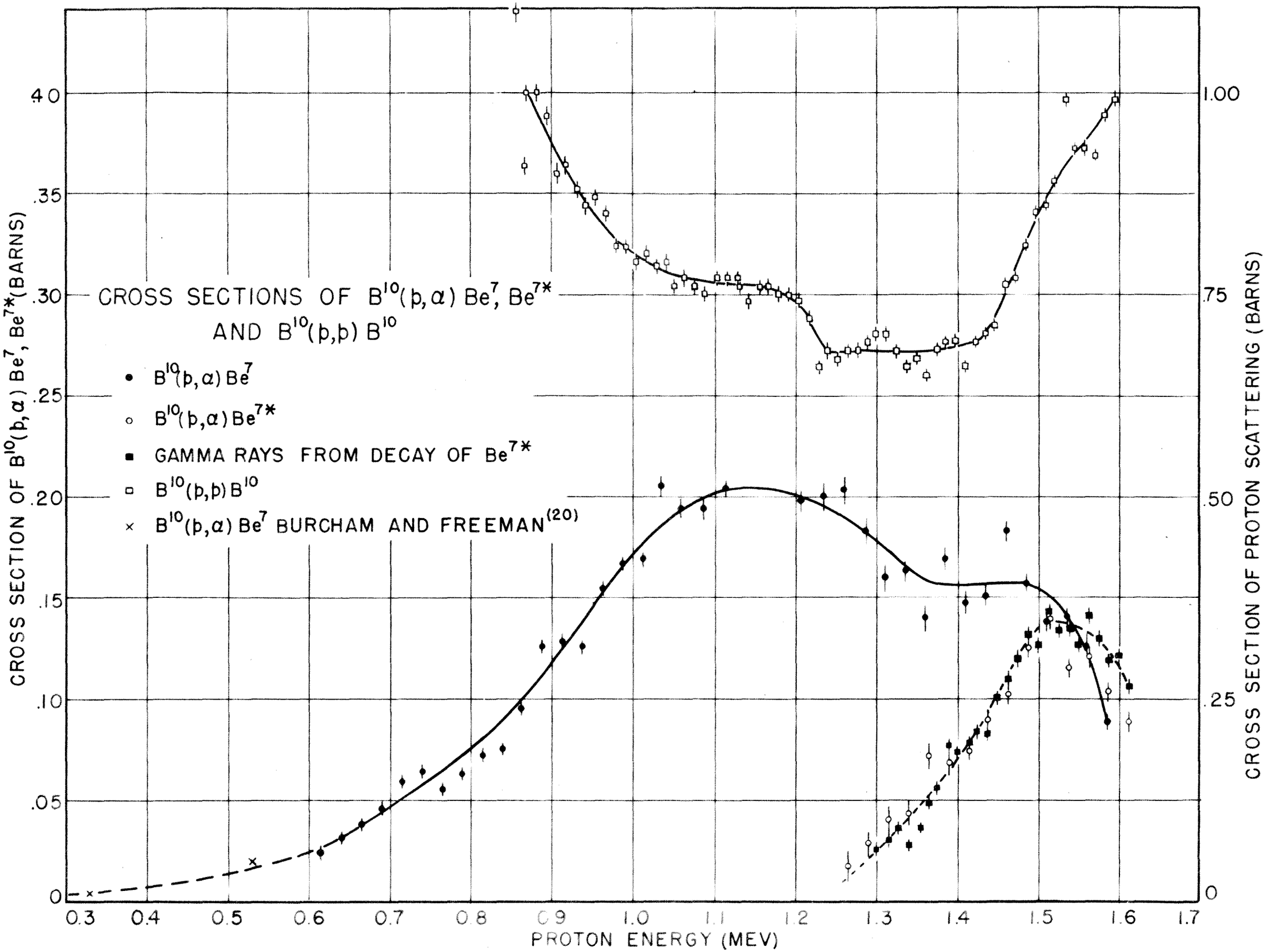
CROSS SECTIONS OF $B^{10}(p,\alpha)Be^{7}$, Be^{7*} AND $B^{10}(p,p)B^{10}$
• $B^{10}(p,\alpha)Be^{7}$
○ $B^{10}(p,\alpha)Be^{7*}$
■ GAMMA RAYS FROM DECAY OF Be^{7*}
□ $B^{10}(p,p)B^{10}$
× $B^{10}(p,\alpha)Be^{7}$ BURCHAM AND FREEMAN[20]
CROSS SECTION OF $B^{10}(p,\alpha)Be^{7}$, Be^{7*} (BARNS)
CROSS SECTION OF PROTON SCATTERING (BARNS)
PROTON ENERGY (MEV)
0
.05
.10
.15
.20
.25
.30
.35
.40
.50
.75
1.00
0.3
0.4
0.5
0.6
0.7
0.8
0.9
1.0
1.1
1.2
1.3
1.4
1.5
1.6
1.7

FIGURE 8

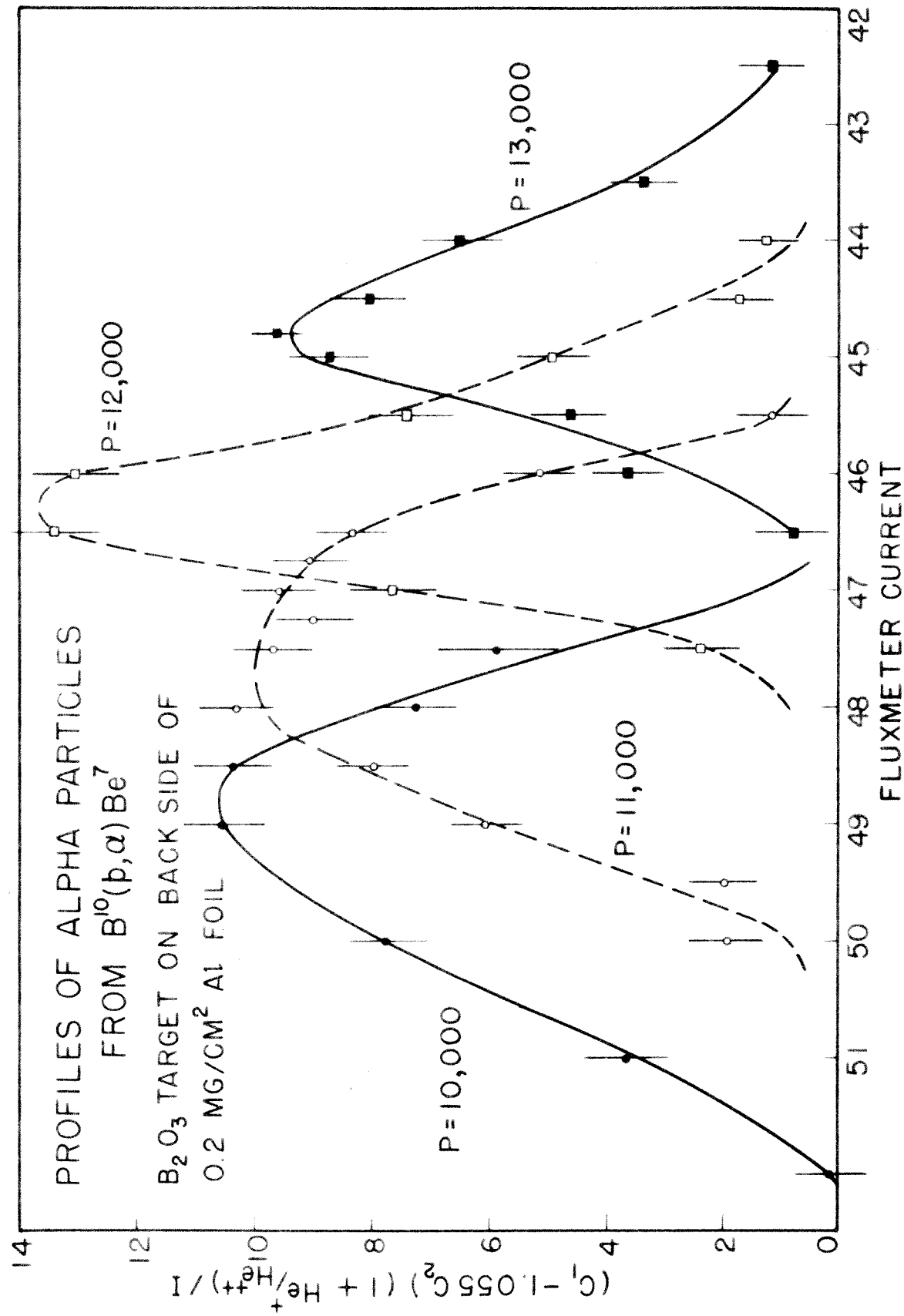
PROFILES OF ALPHA PARTICLES
FROM $B^{10}(b,\alpha)Be^7$
B_2O_3 TARGET ON BACK SIDE OF
0.2 MG/CM² Al FOIL
P=10,000
P=11,000
P=12,000
P=13,000
$(C_1 - 1.055\,C_2)\,(1 + He^+/He^{++})/I$
FLUXMETER CURRENT
0
2
4
6
8
10
12
14
49
50
51
46
47
48
43
44
45
42

FIGURE 9

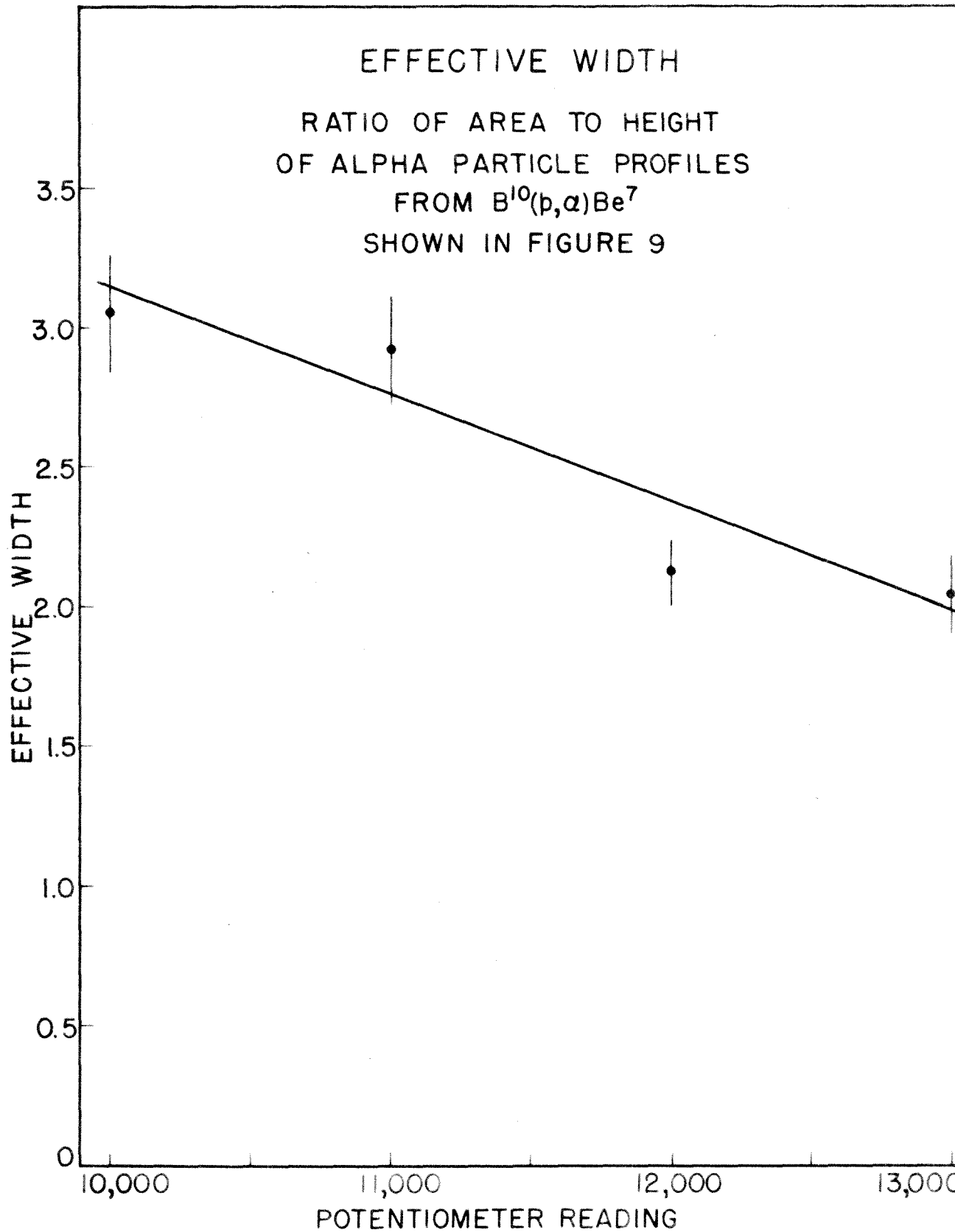
EFFECTIVE WIDTH
RATIO OF AREA TO HEIGHT
OF ALPHA PARTICLE PROFILES
FROM B10(p,α)Be7
SHOWN IN FIGURE 9
EFFECTIVE WIDTH
3.5
3.0
2.5
2.0
1.5
1.0
0.5
0
10,000
11,000
12,000
13,000
POTENTIOMETER READING

FIGURE 10

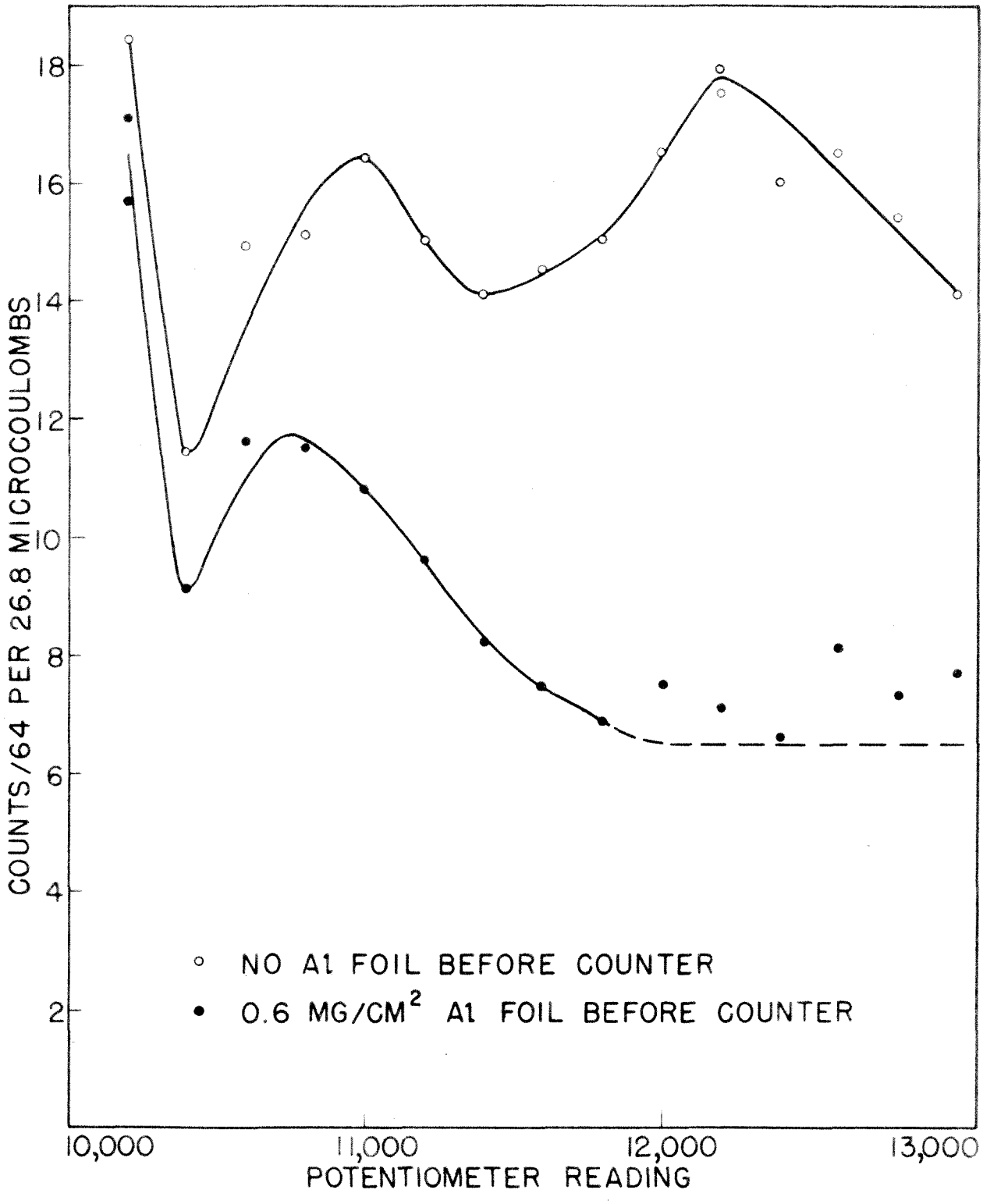

DATA FOR $B^{10}(p,\alpha)Be^{7*}$ CROSS SECTION

FIGURE 11

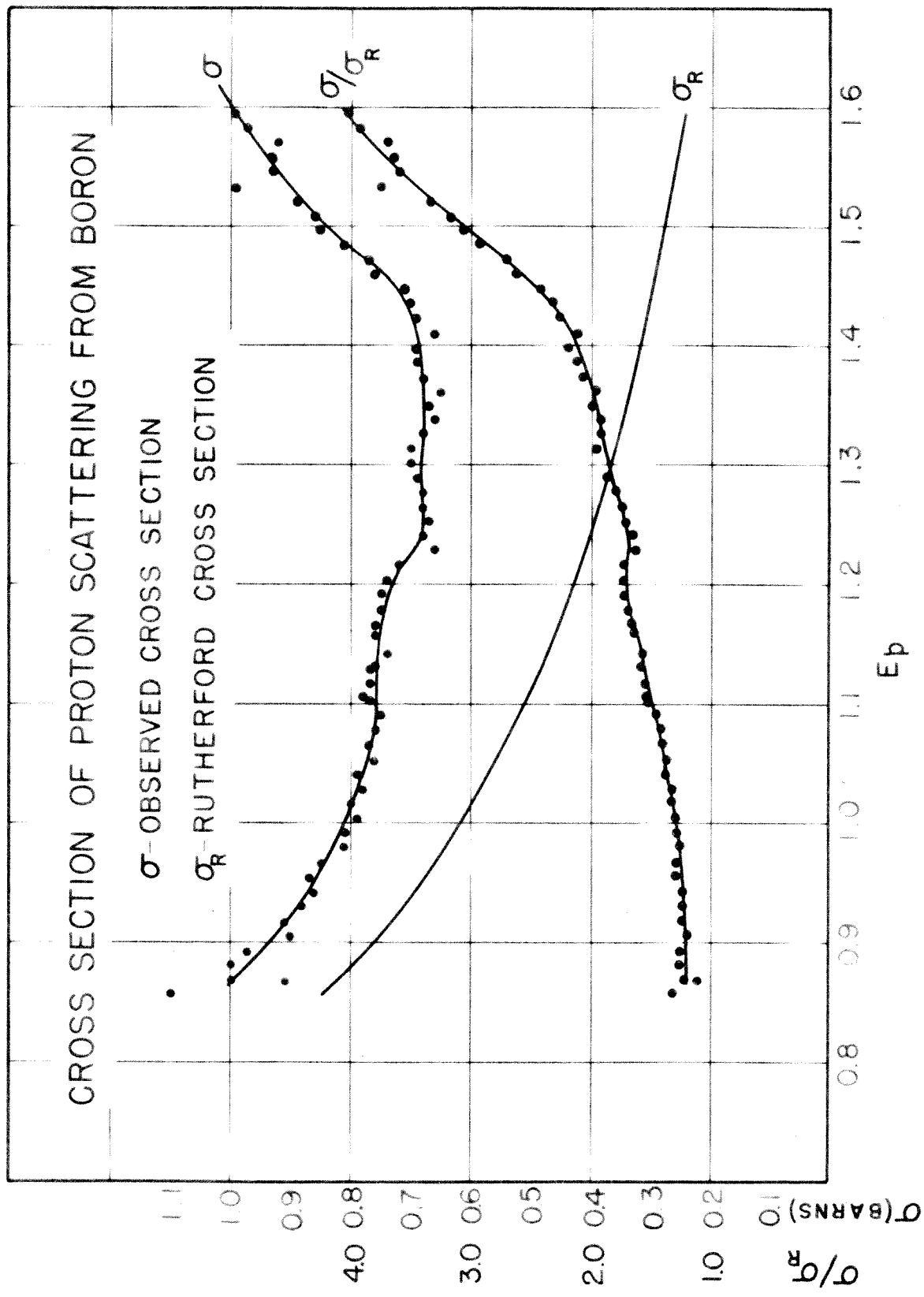
CROSS SECTION OF PROTON SCATTERING FROM BORON
σ-OBSERVED CROSS SECTION
σR-RUTHERFORD CROSS SECTION
σ
σ/σR
σR
σ/σR
σ(BARNS)
Ep
0.8
0.9
1.0
1.1
1.2
1.3
1.4
1.5
1.6
0.1
0.2
0.3
0.4
0.5
0.6
0.7
0.8
0.9
1.0
1.0
2.0
3.0
4.0

FIGURE 12

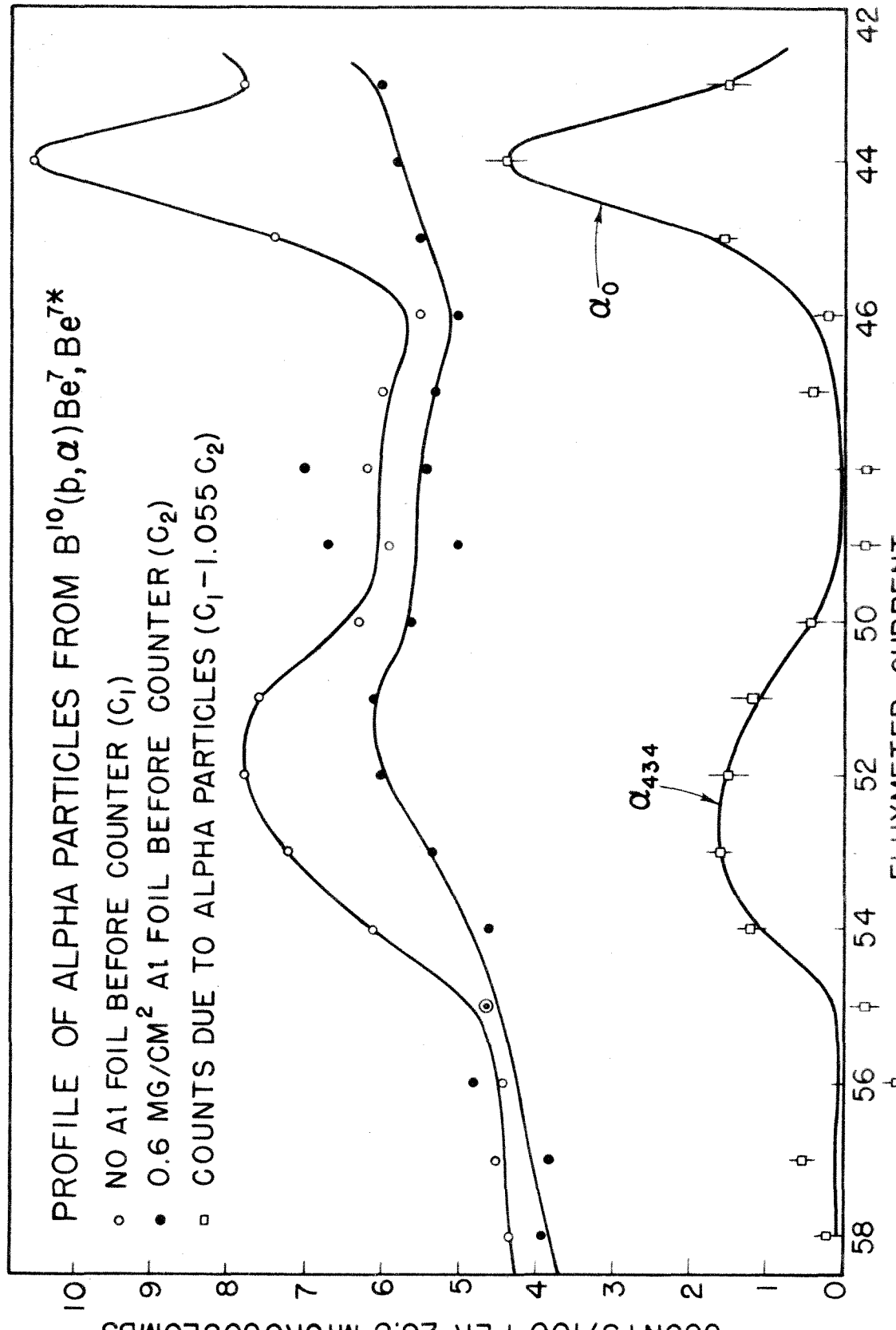
PROFILE OF ALPHA PARTICLES FROM $B^{10}(b,\alpha)Be^7, Be^{7*}$
○ NO Al FOIL BEFORE COUNTER (C_1)
● 0.6 MG/CM^2 Al FOIL BEFORE COUNTER (C_2)
□ COUNTS DUE TO ALPHA PARTICLES ($C_1 - 1.055\,C_2$)
α_{434}
α_0
COUNTS/100 PER 26.8 MICROCOULOMBS
FLUXMETER CURRENT
0
1
2
3
4
5
6
7
8
9
10
42
44
46
50
52
54
56
58

FIGURE 13